In Situ Synthesis of Phenoxazine Dyes in Water: A Cutting-Edge Strategy to "Turn-On" Fluorogenic and Chromogenic Detection of Nitric Oxide

Sébastien Jenni,[#,§,*][a] Kévin Renault,[#,§,*][a] Garance Dejouy,[a] Sylvain Debieu,[a] Myriam Laly,[a] and Anthony Romieu*[a]

[a]   Dr. S. Jenni, Dr. K. Renault, Dr. G. Dejouy, Dr. S. Debieu, Dr. M. Laly, Prof. Dr. A. Romieu
        Institut de Chimie Moléculaire de l'Université de Bourgogne, UMR 6302, CNRS
        Univ. Bourgogne Franche-Comté
        9, Avenue Alain Savary
        21000 Dijon (France)
        E-mail: sebastien.jenni@unige.ch, kevin.renault@unamur.be or anthony.romieu@u-bourgogne.fr

#These authors contributed equally to this work.

§Present addresses: Laboratory of Pharmaceutical Technology, School of Pharmaceutical Sciences, ISPSO, University of Geneva, Rue Michel-Servet 1, CH-1211 Genève, Switzerland (SJ).

                      Département de Chimie, Laboratoire de Chimie Bio-Organique, University of Namur (FUNDP), Rue de Bruxelles 61, Namur B-5000, Belgium (KR).

Abstract: The synthesis of phenoxazine dyes was revisited in order to access these fluorescent N,O-heterocycles under mild conditions. The combined sequential use of nitrosonium tetrafluoroborate (NOBF$_4$) and triphenylphosphine enables the facile conversion of bis(3-dimethylaminophenyl) ether into the methyl analog of popular laser dye oxazine 1. The ability of nitrosonium cation (NO$^+$) to initiate the domino reaction resulting in π-conjugated phenoxazine molecules under neutral conditions, then led us to explore the feasibility of expanding it in aqueous media. Thus, we explored the use of reactive signaling molecule nitric oxide (NO) as a biological trigger of phenoxazine synthesis in water. The implementation of a robust analytical methodology based on fluorescence assays and HPLC-fluorescence/-MS analyses, have enabled us to demonstrate the viability of this novel fluorogenic reaction-based process to selectively yield an intense "OFF-ON" response in the near-infrared (NIR-I) spectral region. This study is an important step towards the popularization of the concept of "covalent-assembly" in the fields of optical sensing, bioimaging and molecular theranostics.
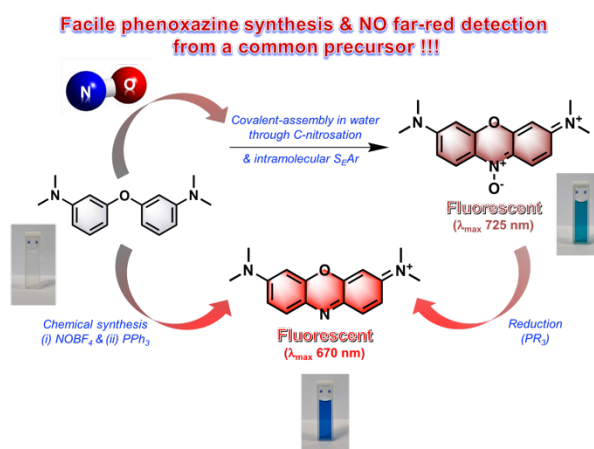
Keywords: covalent-assembly • domino reactions • fluorescent probe • nitric oxide • phenoxazine dyes

Introduction

Phenoxazine dyes, formally defined as anthracene analogs in which the middle ring is replaced by a morpholine unit, are an important class of heterocycles, mainly explored both for their biological activities and their ability as high-performance biological staining agents.[1] Among the myriad of synthetic compounds belonging to the phenoxazine family, those decorated with a pair of electron-donating and -withdrawing groups as substituents (*i.e.*, push-pull substituents) and/or structurally fused with a further benzene ring (*e.g.*, "angular" or "linear" benzophenoxazines)[2] for elongation of their π-conjugated system, often exhibit good fluorescence within the orange-red spectral range or beyond 650 nm in the first near-infrared (NIR-I) region.[3] This emissive capability is characterized by the following features: high quantum yields mainly in non-polar solvents, large Stokes' shifts and a high sensitivity to the surrounding environment (polarity, viscosity, ...) leading to marked solvatochromism. The most popular phenoxazine-based fluorophores are Nile Red, Nile Blue, Cresyl Violet and its non-methylated analog Oxazine 9 (Figure 1). The latter ones and close structural analogs are used for the most demanding fluorescence-based biosensing/bioimaging applications.[4] Indeed, they take advantage of their unique ability to be used either as non-covalent labeling agents highly selective for some biological structures/assemblies (*e.g.*, membranes and lipid microdomains[5], amyloid fibrils[6], DNA[7] and related unusual nucleic acids structures such as G-quadruplexes[8]) or as reactive fluorescent labels if a bioconjugatable handle is available within their core structure. Furthermore, the presence of a primary aniline moiety or the possible introduction of an additional phenol, both acting as

effective optically tunable groups, imparts these molecules fluorogenic reactivity, which is of primary importance for designing reaction-based small-molecule fluorescent probes. Thus, the probe design strategy based on protection-deprotection of an amino or hydroxyl group[9] was successfully applied especially to the detection of biologically relevant analytes including enzymatic biomarkers, biomolecules (e.g., biothiols) and gasotransmitters, most often through an intensometric "OFF-ON" response.[10] Interestingly, analyte- or environment-assisted modulation of other photophysical processes such as Förster resonance energy transfer (FRET) or through-bond energy transfer (TBET) has also been regarded for biosensing/biomaging operations based on the use of "smart" phenoxazine reporters.[11] Other benefit of these probe developments is related to the major advances made in the chemistry of parent fluorophores aimed at improving their spectral features, bioconjugation ability, water solubility and cell permeation or amphiphilic character and targeting properties. Major contributions in this field, notably from the Belov-Hell[12], Burgess[13], Gonçalves[14], Klymchenko[5] and Mılller[15] groups are worthy of note.

Inspired by the conventional synthetic methods typically used for preparing (benzo)phenoxazine derivatives and based on an acid-catalyzed condensation reaction between a nitroso intermediate and an electron-rich aromatic compound (typically, a phenylogous amine or a phenol) as the key step, the Yang group has explored a new probe design principle, namely the "covalent-assembly" approach[16], for detecting ROS/RNS through in situ formation of fluorescent phenoxazine dyes or related analogs (i.e., coumarin-resorufin fused compounds)[17] (Figure 2). The positive attributes of this novel class of activatable fluorescent probes relating to their ability to dramatically improve signal-to-noise ratio (S/N) responses, and hence to provide optimal detection sensitivity, led us to devise a novel water-compatible cascade reaction triggered by an enzyme (i.e., penicillin G acylase (PGA) used as model protease) and potentially producing fluorescent 9-amino-5H-benzo[a]phenoxazin-5-one (Figure 2). Indeed, this is a vital step towards applying the "covalent-assembly" principle to in vivo medical diagnostics through the use of "smart" NIR-I fluorescent imaging agents activated by disease-associated enzymes or other reactive biomarkers.[18] However, in vitro enzymatic assays conducted with PGA-sensitive dual-reactable probe 1 and based on fluorescence measurements and HPLC-MS analyses have not enabled us to demonstrate the assumed reaction-based sensing mechanism. Indeed, PGA failed to hydrolyze the second triggering unit phenylacetamide and two distinct compounds 2 and 3, that differ structurally from the expected fluorophore, have been identified. Possible structures based on an unusual fused four-ring heterocyclic system named 11a,12-dihydro-11H-benzo[b]phenoxazine-6,11(5aH)-dione, have been proposed (Figure 2). To overcome this major bottleneck associated with the application of "covalent-assembly" probe design principle to (benzo)phenoxazine dyes, we brainstormed on a different strategy that takes advantage of water-compatible reactions that have already proven successful in this context, and reported by Yang and Anslyn[19], and our group[20]: (1) effective nitrosation of anilines or electron-rich aromatic derivatives with dinitrogen trioxide (N2O3), the oxidized surrogate of important biologically produced gasotransmitter nitric oxide (NO), and (2) facile ring closure of mixed biphenyl derivatives or bis-aryl ethers through an intramolecular electrophilic aromatic substitution (SEAr) reaction involving a phenylogous amine. We have therefore hypothesized that NO+ or N2O3 could trigger in situ formation of phenoxazine

dyes from readily accessible symmetrical bis-aryl ethers, under aqueous conditions, and through a novel domino process involving aromatic C-nitrosation followed by intramolecular nucleophilic addition of the adjacent phenylogous amine. We assume that N-oxide phenoxazine formed may be fluorescent and/or prone to biological reduction[21] to give the targeted far-red emitting phenoxazine dye (Figure 3).

Herein, we report the practical implementation of this unprecedented fluorogenic cascade reaction with the dual aim of expanding the scope of "covalent-assembly" principle to long-wavelength fluorophores and establishing a novel and effective sensing scheme for NO. The versatility of this approach was also examined by considering several phenoxazine precursors that differ from each other through the nature of their electron-donating dialkylamino groups or by the presence of a dimethylsilicon moiety instead of the bridging oxygen atom. Indeed, these structural modifications are often applied to different classes of organic-based fluorophores (e.g., phenoxazines[15b, 22], rhodamines[23],[24], ...), to improve and red-shift their spectral properties. In addition to these synthetic aspects, a set of in vitro fluorescence assays and HPLC-fluorescence-/-MS analyses was undertaken to study in detail NO-mediated construction of phenoxazine dyes.

Results and Discussion

As briefly mentioned above, the traditional synthetic method often employed for preparing common angular phenoxazine dyes (i.e., Nile Red and Nile Blue derivatives) is based on an acid-mediated condensation reaction between a nitrosylated aminophenol and an hydroxy- or aminonaphthalene, conducted under harsh conditions (i.e., conc. HCl, polar solvent such as EtOH or DMF heated under reflux or at 80-90 °C respectively).[3] Our proposed approach distinguished by the implementation of a NO-mediated cyclization process as the key synthetic step, may offer distinct advantages including milder reaction conditions (vide infra) and the use of a structurally simple symmetrical bis-aryl ether as a "covalent-assembly" precursor of phenoxazine. Our initial efforts were then devoted to the synthesis of such aromatic ethers and a hetero-analog in which the bridging oxygen atom is replaced by the dimethylsilicon moiety.

Synthesis of symmetrical bis-aryl ethers and a silicon-containing analog

The straightforward synthetic route employed for the rapid preparation of bis(3-dimethylaminophenyl) ether 4 is based on a copper-catalyzed Ullmann-type C-O cross-coupling reaction between 3-(dimethylamino)phenol and 3-bromo-N,N-dimethylaniline, conducted under conditions historically proposed by the Cornish group[25] and recently optimized by us to readily obtain precursors of pyronin dyes[26] (Scheme 1). The use of a commercially available bromoarene as electrophilic coupling partner instead of its iodo counterpart (whose synthetic accessibility requires formal N,N-dimethylation of commercial 3-iodoaniline) has not given rise to any major problems of reactivity and the desired phenoxazine precursor 4 was obtained with a satisfying but not optimized 75% yield. For the purpose of possibly improving kinetics of the NO-triggered "covalent-assembly" process and optimizing photophysical properties of in situ formed

2

phenoxazine (*i.e.*, red-shifting of absorption/emission maxima and enhancement of fluorescence quantum yield) through a molecular rigidification approach, the synthesis of symmetrical bis-aryl ether **5** bearing two julolidine units was also attempted. Nevertheless, despite several attempts for which the copper source, the ligand, the base and the solvent were varied, this Ullmann coupling product was never detected from RP-HPLC-MS analyses of the reaction mixtures. We also noted the degradation of starting 8-hydroxyjulolidine. We assume a lack of reactivity of 8-bromojulolidine that is electron-enriched compared to 3-bromo-N,N-dimethylaniline, as a result of the greater electron-donating ability of its dialkylamino group than that of dimethylamino moiety. Furthermore, to the best of our knowledge, the iodo counterpart, perhaps more reactive in this context, has never been reported and its synthetic accessibility seems to be not a trivial task.

Since a reliable and effective synthetic route to obtain the silicon analog of bis(3-dimethylaminophenyl) ether (diaryl ether analog **6**, recently abbreviated by Deng *et al.* DAEA-Si) has already been devised and reported in the literature[27], no improvement has been made by us in the practical implementation of lithium-halogen exchange reaction between 3-bromo-N,N-dimethylaniline and *n*-BuLi, and subsequent silylation with Me_2SiCl_2. DAEA-Si **6** was obtained in a pure form after conventional flash-column chromatography over silica gel (yield 39%).

Mild condition synthesis of phenoxazine dye 8 and its silicon analog 10 through nitrosation in an organic medium

The bench-stable, commercially available nitrosating agent, nitrosonium tetrafluoroborate ($NOBF_4$)[28] has been recently used for the facile synthesis of aromatic azo compounds under mild conditions particularly well-suited for reactions involving highly functionalized tertiary anilines as coupling partners.[29] Surprisingly, to the best of our knowledge, $NOBF_4$ has still not be used as the source of nitrosonium (NO^+) cation in the synthesis of (benzo)phenoxazine dyes. In order to demonstrate that this electrophilic species is able to trigger the phenoxazine dyes synthesis *in situ*, under neutral mild conditions, bis(3-dimethylaminophenyl) ether **4** was reacted with 1 equiv. of $NOBF_4$, in MeCN at room temperature (Scheme 2). The complete consumption of starting **4** was observed within only 5 min and formation of a deeply blue-green colored compound identified as N-oxide phenoxazine dye **7** was observed. Isolation of this unprecedented aminated analog of resazurin (**RZ**), N-oxide derivative of resorufin (**RF**) and currently used as indicator of cell viability[30], was achieved by conventional flash-column chromatography over silica gel (isolated yield 25%). This modest but not optimized yield can be explained by the presence of nitronium tetrafluoroborate (NO_2BF_4) in the old batch of $NOBF_4$ used, leading to undesired nitration reactions of **4**. Yield improvement can be achieved using a fresh bottle of $NOBF_4$. Deoxygenation of this N-oxide was readily achieved using a slight excess of triphenylphosphine (1.2 equiv.) in MeCN at room temperature[31], to give 3,7-bis(dimethylamino)phenoxazin-5-ium dye **8**. Purification by semi-preparative RP-HPLC has enabled its isolation in a pure form and as TFA salt (isolated yield: 65%). All spectroscopic data, especially NMR and mass spectrometry data, were in agreement with the two structures assigned. The quantitative determination of fluorophore counter-ion (1x tetrafluoroborate BF_4^- and 2.37x trifluoroacetate $CF_3CO_2^-$ for **7** and **8** respectively) was achieved by ionic chromatography. The

purity of both compound (determined through RP-HPLC analyses at different wavelength channels) was found to be equal to or above 97%, and thus being suitable for the reliable study of their photophysical properties. From a mechanistic point of view, we assume that NO^+ ion readily reacts with one of the two identical electron-rich benzene unit of **4**, through a conventional electrophilic aromatic substitution (S_EAr) reaction (Figure 3). The regioselectivity of this step was governed by the strong electron-donating ability of dimethylamino group and functionalization only at the C-6 position (*i.e.*, para position relative to $-NMe_2$ group) was observed. The nitroso intermediate may have to undergo intramolecular nucleophilic attack of the adjacent phenylogous dimethylamino unit, to give after abstraction of the ring junction proton, N-oxide phenoxazine dye **7**.

Backed by this first success in the direct and facile synthesis of long-wavelength fluorophores from a structurally simple bis-aryl ether, we next examined the preparation of red-shifted silicon analog **10** from DAEA-Si **6**[27]. However, the reaction between this dimethyldiarylsilane and $NOBF_4$ conducted under the same non-acidic conditions, did not provide the desired N-oxide Si-oxazine dye (azasiline dye) but a mixture of nitroso and nitro derivatives of starting compound. The tetrahedral geometry around the silicon atom of **6** and the longer C-Si bond length are unlikely to favor the intramolecular bridging reaction between the nitrosoaryl and phenylogous amine moieties in contrast to what was occurred with bis-aryl ether **4**.[15b]

Photophysical properties of phenoxazine dye 8 and its N-oxide derivative 7

The electronic absorption and fluorescence spectra of phenoxazine dye **8** and its N-oxide parent compound **7** were recorded in DMSO (as a representative polar organic solvent), and in several different aqueous media (*i.e.*, ultrapure water, 0.1% aq. formic acid pH 2.1, 50 mM HEPES buffer pH 7.4) used in the *in vitro* fluorescence assays and HPLC-fluorescence/-MS analyses in place to demonstrate fluorogenic detection of NO *via* the "covalent-assembly" principle (see next section). Table 1 summarizes the corresponding spectral features and overlay of the normalized absorption/excitation/emission spectra in DMSO and water are displayed in Figure 4. Not surprisingly, whatever the polar medium used, and by analogy with popular laser dye oxazine 1 (also known as oxazine 725, **Ox-1**)[32], **8** displays a broad and intense absorption band in the visible region of the spectrum with a maximum close to 650 nm, and assigned to the 0-0 band of the S_0-S_1 transition (electronic transition of π-π^* type). The short-wavelength shoulder at $\lambda \approx 600$ nm has a vibronic origin (*i.e.*, the sum of the vibronic subbands of the S_0-S_1 transition). The alternative hypothesis to explain the shape of this absorption band, linked to the formation of non-emissive aggregates (*i.e.*, H-type homodimers), is absolutely excluded. Indeed, a perfect matching between the absorption and excitation spectra of **8** recorded in DMSO or aq. buffers, for concentrations within the range 5-20 μM, is observed (Figure 4). Excitation at 600 nm leads to an intense far-red emission band centered at 666-676 nm. Values of fluorescence quantum yield in polar protic media (determined using Nile Blue in EtOH as standard, $\Phi_F = 27\%$, see Table 1) are comparable to that of **Ox-1** in EtOH, and as expected, a significant increase was obtained in the higher-viscosity solvent DMSO.

Table 1. Photophysical properties of phenoxazine dyes and related compounds at 25 °C.

Dye[a]	Solvent	Abs max[b] [nm]	Em max [nm]	Stokes shift [cm^{-1}]	ε [M^{-1} cm^{-1}]	Φ_F[c] [%]
7	DMSO	407, 683	726	10 796, 867	7 800 63 300	12
	H$_2$O	403, 685	726	11 040, 824	6 950, 59 200	3
	aq. 0.1% FA (pH 2.1)	403, 686	728	11 078, 841	7 150, 58 900	2
	aq. HEPES (pH 7.4)	402, 684	725	11 021, 827	7 100, 60 350	3
8	DMSO	654	676	498	119 400	27
	H$_2$O	648	668	462	118 000	0.11
	aq. 0.1% FA (pH 2.1)	648	666	417	121 700	11
Ox-1	EtOH[d]	646	663	397	118 800	14
RZ	aq. NaOH (pH 9.5)[e]	602	634	838	47 000	11
RF	aq. NaOH (pH 9.5)[e]	572	585	388	56 000	74

[a] Stock solutions (1.0 mg/mL) of fluorophores prepared in DMSO. [b] Only 0-0 band of the S$_0$-S$_1$ transition of phenoxazine unit is reported only for **8**. [c] Determined using an aza-BODIPY dye (Φ_F = 36% in CHCl$_3$, Ex at 630 nm) or Nile Blue (Φ_F = 27% in EtOH, Ex at 600 nm) as a standard[33]. [d] Values determined and reported by Rurack and Spieles[32]. [e] Values determined and reported by Bueno *et al.*[34]

By analogy with its phenolic analog **RZ**[34], the UV-visible absorption spectra of N-oxide derivative **7** consist of an intense band at ca. 685 nm and a weak band at ca. 400 nm respectively assigned to π-π* transition of the phenoxazine ring system and n-π* transition of N-oxide moiety. Interestingly, the large change in absorption features between this compound and its reduced form **8** enables their facile naked-eye distinction, especially in aq. solution (blue-green and cyanine 5 blue color respectively, see Figure S1). Furthermore, a marked bathochromic shift (ca. +50 nm) in emission maximum and a decrease of fluorescence quantum yield (determined using an aza-BODIPY dye in CHCl$_3$ as standard, Φ_F = 36%, see Table 1) are also obtained whatever the polar solvent used. However, it is interesting to note that this far-red fluorescence decline is much less important than the one reported for the pair **RF-RZ** (see Table 1). Gratifyingly, this study has enabled us to identify a novel NIR-I fluorescent organic dye with valuable features: compact structure and small molecular weight, low hydrophobicity and resistance to aggregation in aq. solutions, despite a modest brightness value. If we are completely honest, we must also mention that a slow degradation of this N-oxide-based fluorophore was noted during its prolonged solid-state storage at 4 °C (ca. 10% of degradation based on a RP-HPLC analysis after 12 months) to give several unidentified products lacking absorption within the visible spectral range. This latter point suggests a degradation pathway involving a ring-opening process and leading to disruption of the π-conjugation of the phenoxazine chromophore. This hypothesis will be strengthened by further investigations aimed at characterizing spectrospically the degradation products.

Wet synthesis of phenoxazine dye 8 and its N-oxide derivative 7. "Turn-on" fluorogenic detection of NO

In addition to its marked reactivity towards nitrosating agents (*vide supra*), the lack of both visible color absorbance and fluorescence properties for diaryl ether analog **4** then led us to evaluate this structurally simple molecule as a zero-background fluorescent probe for gasotransmitter NO. This ubiquitous cellular signaling molecule is involved in various metabolic pathways and its abnormal levels are often associated with pathological states of various diseases (*e.g.*, cardiovascular diseases[35], asthma, cancer, neurodegenerative disorders, ...). Consequently, due to this pivotal role, several direct or indirect methods for detecting and quantifying NO levels in different biological matrices have been developed. Among these, those based on electrochemical, optical and/or nanoscale sensors/probes are often regarded as promising approaches for accurate and real-time bioimaging of NO, with the aim of facilitating robust biomedical or clinical translational applications (*i.e.*, clinical diagnostics).[35] In the field of small-molecule fluorescent probes responsive to this gasotransmitter[36], a major breakthrough was achieved by Anslyn and Yang through the design of highly selective low-background imaging agents based on the "covalent-assembly" principle (see introduction section and Figure 2). Indeed, they discovered that non-emissive 2-aminobiphenyl scaffolds were able to selectively create green-yellow-emitting fluorophores based on benzo[c]cinnoline heterocycle, upon their reaction with N$_2$O$_3$ (oxidized surrogate of NO) and under physiological conditions.[19a-c] However, despite a comprehensive structure-property relationship study aimed at optimizing spectral properties of *in situ* formed benzo[c]cinnoline derivative, they did not manage to identify a candidate suitable for *in vivo* detection of NO within the NIR-I spectral region. In order to fill this gap and to rapidly establish a proof-of-concept, we wished to study the fluorogenic behavior of bis(3-dimethylaminophenyl) ether **4** in the presence of gasotransmitter NO. From a practical point of view, a fresh aq. solution of NO was prepared using a literature procedure and its concentration was determined to be 10.7 mM by the Griess method[37]. Fluorogenic NO assays and blank experiments were achieved through time-course measurements. Ultrapure water was chosen as aq. medium because our preliminary attempts conducted with phosphate buffer (PB, 100 mM, pH 7.6) or HEPES buffer (50 mM, pH 7.4) failed undoubtedly by virtue of a too rapid degradation of NO. As shown in Figure 5A and unsurprising, probe **4** displayed an ultra-low background fluorescence, typical of xanthene-based "covalent-assembly" fluorescent probes; upon incubated with different amounts of NO (25 to 300 equiv.), a dramatic and gradual increase of NIR-I fluorescence signal was observed, indicating the continuous incremental formation of N-oxide derivative **7** in solution (Ex/Em 685/730 nm). Furthermore, a good overlay between the emission spectrum of solution, recorded after 25 min of incubation with NO, and the emission curve of pure fluorophore independently synthesized through the NOBF$_4$ procedure (*vide supra*), was obtained (Figure 5B). This positive result supports our initial hypothesis whereby *in situ* formation of a phenoxazine core is able to take place in water, initially triggered by NO-mediated C-nitrosation and completed by an electronic cascade involving the phenylogous amine (Figure 3). Depending on the excess of the nitrosating agent added to the

aq. solution of **4**, the plateau was reached within a time range of 10 to 20 min. An additional spectroscopic evidence of the effective synthesis of this fluorescent heterocycle in water, was the rapid coloration of the probe solution in blue-green upon addition of reactive analyte (see Figure S1). Therefore, this probe design principle may also be applicable to chromogenic "naked eye" detection of NO or related nitrosating agents. Since heterocyclic N-oxide derivatives are known to be prone to facile reduction (*i.e.,* deoxygenation), we actually think that *in situ* formed fluorophore **7** could be wholly or partly converted into phenoxazine **8** depending on the redox status of the medium in which its NO-sensitive precursor **4** would be used.[21] Consequently, a dual-channel fluorescence detection/imaging scheme should be preferred for the simultaneous visualization of the two emissive species possibly formed. To verify both formation of phenoxazine **8** under mild reducing conditions and the possibility of its real-time detection using a more suitable set of Ex/Em parameters (Ex/Em 650/675 nm), we performed further kinetic experiments involving one-pot sequential incubation with NO (50 equiv., 25 min of incubation) and a water-soluble reductant (*i.e.,* tris(2-carboxyethyl)phosphine (TCEP) 170 equiv., or NADH 140 equiv.). The spectral changes observed on both N-oxide and phenoxazine channels (Figure 6), when "covalent-assembly" type probe **4** was subjected successively to the nitrosating agent and phosphine, clearly confirm the facile reduction of **7** and its conversion into phenoxazine **8**. Indeed, over the course of 10 min, the fluorescence emission intensity at 730 nm steadily decreased and that centered at 675 nm steadily increased. More disappointing results were obtained from experiments conducted with NADH because fluorescence time-course measurements reveal chemical inertness of N-oxide derivative **7** towards this biocompatible hydride source, at least in the non-buffered conditions chosen for our *in vitro* validations. To confirm that fluorescence signal changes observed during the activation kinetics of probe **4** were due to the *in situ* formation of phenoxazine heterocycles **7** and **8**, each reaction mixture was subjected to RP-HPLC-fluorescence analyses (Figure 7 for selected examples). For each sample collected from the reactions with NO alone, a single peak was detected (t_R = 3.45 min) on the channel Ex/Em 685/730 nm, and unambiguously assigned to the expected N-oxide fluorophore (co-injection with an authentic sample of **7**). Interestingly, a second peak with a lower retention time (t_R = 3.36 min) was observed but only on the phenoxazine channel Ex/Em 650/675 nm, and identified as being the deoxygenated analog (again, through co-injection with an authentic sample of **8**). It may be surprising to detect phenoxazine **8** in mixtures not containing a reducing agent even its formation rate is limited. One hypothesis based on a photoreduction process promoted by the long-time irradiation required for kinetics measurements, can be put forward to explain the unexpected formation of **8**.[38] Furthermore, since the fluorescence quantum yield of this fluorophore is much higher than that of its N-oxide precursor **7**, detection on channel Ex/Em 650/675 nm was dramatically maximized. For kinetics involving sequential incubations of **4** with NO and TCEP, the disappearance of N-oxide peak at t_R = 3.45 min and the increase of phenoxazine peak height (t_R = 3.36 min) were observed. These results are fully consistent with those arising from fluorescence time-course measurements and confirm the facile deoxygenation of **7** under mild aq. reducing conditions. Finally, in order both to provide a further evidence for the claimed detection mechanism and to evaluate the conversion rate of the fluorogenic cascade reaction occurring in pure water,

the same mixtures were analyzed by RP-HPLC-MS (Figure 8 for selected examples). Several valuable observations and conclusions have been drawn: (1) the disappearance of the starting "covalent-assembly" probe **4** peak (t_R = 4.22 min) is clearly observed whatever the excess of NO used, thus confirming the high reactivity of this diaryl ether analog towards this nitrosating reagent; (2) the formation of several products, the three main ones being the targeted N-oxide phenoxazine dye **7** (t_R = 3.44 min, λ_{max} = 679 nm, MS(ESI+): *m/z* = 284.3 [M]$^+$, calcd for $C_{16}H_{18}N_3O_2^+$ 284.1) and two isomeric bis-nitro derivatives of bis(3-dimethylaminophenyl) ether (t_R = 5.04 and 5.28 min, λ_{max} = 396 and 438 nm, MS(ESI+): *m/z* = 347.0 [M + H]$^+$, calcd for $C_{16}H_{19}N_4O_5^+$ 347.1) showing that NO-mediated nitrosation reaction is not univocal and therefore that the phenoxazine-based fluorophore scaffold construction is not a quantitative process. The same analytical methodology applied to samples having undergone a further reduction step also provided interesting mechanistic information (Figure 9 for selected examples). Indeed, as expected, incubation with a large excess of TCEP resulted in disappearance of the peak of N-oxide **7** and appearance of a new one at t_R = 3.35 min unambiguously assigned to phenoxazine dye **8** (λ_{max} = 646 nm, MS(ESI+): *m/z* = 268.3 [M]$^+$, calcd for $C_{16}H_{18}N_3O^+$ 268.1). Interestingly, the analysis of some crude nitrosation/reduction reaction mixtures also revealed the lack of phenoxazine dye **8** and the presence of a more polar compound (t_R = 2.25 min) with the following spectroscopic signature: λ_{max} = 652 nm, MS(ESI+): *m/z* = 516.4 [M^{2+} - H]$^+$ and 258.8 [M]$^{2+}$, calcd for $C_{25}H_{32}N_3O_7^{2+}$ 517.2, was observed (Figure 9). This compound was assigned to a covalent adduct between fluorophore and TCEP, probably formed through a nucleophilic addition of this phosphine to the *N*-(4-imino-2,5-cyclohexadien-1-ylidene)-*N*-methylmethanaminium ring moiety of **8** followed by spontaneous oxidation to reform the π-conjugated system of phenoxazine dye. Even if this phosphonium-based phenoxazine derivative has not yet independently synthesized and its spectral properties determined, we assume that this compound keeps fluorescence properties because it was possible to detect it on the phenoxazine Ex/Em 650/675 nm channel used for RP-HPLC-fluorescence analyses. To the best of our knowledge, this type of oxidative addition reaction has never been studied extensively in the context of phenoxazine dyes, except in the case of resorufin derivatives. Indeed, covalent adducts with β-mercatpoethanol and enzymes (*e.g.,* sheep liver cytosolic aldehyde dehydrogenase) have been synthesized and fully-characterized, and mechanistic insights into their formation have been gained.[39]

All the collected data allowed us to confirm the viability of the NO-sensing mechanism initially claimed even if the novel "covalent-assembly" strategy producing far-red/NIR-I active phenoxazine scaffolds, is not a quantitative process, at least, in the selected *in vitro* conditions. Indeed, NO spontaneously reacts with triplet oxygen to produce a myriad of reactive nitrogen species (RNS) and some of them may be able to nitrate bis-aryl ether **4**, these reactions being concurrent to the desired nitrosation process as evidenced by RP-HPLC-MS analyses (*vide supra*). More broadly in the field of reaction-based fluorescent probes, the analytical methodology used above illustrates the need and the utility to systematically combine conventional fluorescence-based assays with complementary HPLC-fluorescence and HPLC-MS analyses, for deciphering precisely the activation mechanism of such sensing molecular tools based on fluorescence modality.

Conclusions

In summary, we developed a novel straightforward synthesis of phenoxazine dyes, whose usefulness was illustrated through rapid access to the methyl analog of NIR-I fluorophore oxazine 1 from bis(3-dimethylaminophenyl) ether **4**. Compared to synthetic methods commonly employed for preparing these fluorescent N,O-heterocycles, the main improvement is the use of NOBF$_4$ as nitrosating agent, that facilitates the construction of phenoxazine scaffold under mild neutral conditions and *via* an N-oxide intermediate; this latter one undergoing a smooth reduction with a phosphine. Therefore, it was easy to implement this domino process in pure water using nitric oxide and a water-soluble phosphine TCEP as biocompatible trigger and reductant respectively. Since both reactions (*i.e.*, nitrosation/cyclization and deoxygenation of heteroyclic N-oxide) cause dramatic changes in the spectral properties of starting non-fluorescent and UV-absorbing diaryl ether analog **4**, these could be advantageously utilized for construction of high-performance "OFF-ON" fluorescent probes for monitoring NO in living biological systems. Depending on the cellular redox state, and possible interactions of NO with biologically relevant thiols (*i.e.*, cysteine, homocysteine and glutathione)[40], a dual-channel fluorescence signal readout strategy based on simultaneous or sequential detection of N-oxide **7** and phenoxazine **8**, will be considered.[41] Within this context, our work is the first example of "covalent-assembly" type probe that yields far-red/NIR-I fluorescent molecules in water and through an intramolecular cascade reaction triggered by a biorelevant analyte (or at least, its oxidized surrogate N$_2$O$_3$). Interestingly, during the course of our study, another "covalent-assembly" approach for NIR-I fluorescence sensing of nerve agent mimic diethyl chlorophosphate (DCP) in organic media (DMSO) was proposed by Vijay *et al.*[42] Indeed, *in situ* formation of a coumarin fused pyronin hybrid dye from a 4-aryloxy derivative of 7-(diethylamino)-3-formylcoumarin, through a chemical cascade triggered by DCP, causes large bathochromic shifts in both absorption (from 263/368 nm to 600 nm) and emission maxima (from 585 nm to 658 nm), enabling the rapid and facile ratiometric detection of this electrophilic phosphorus compound in various matrices including soil samples and living cells (Figure 10). These two pioneering contributions show quite clearly the potential benefits to be gained by designing NIR-I "covalent-assembly" fluorescent probes and should therefore stimulate research efforts in this direction. To achieve this ambitious goal, organic chemists will have a key role to play, through the discovery of novel cascade chemical transformations, often biocompatible and leading to π-extended push-pull molecules.

Experimental Section

General
Unless otherwise noted, all commercially available reagents and solvents were used without further purification. TLC was carried out on Merck Millipore DC Kieselgel 60 F-254 aluminum sheets. The spots were directly visualized or through illumination with a UV lamp (λ = 254/365 nm). Purifications by flash-column chromatography were performed on silica gel (40-63 µm) from VWR. Acetonitrile (MeCN, RE grade, #P0060268) from Carlo Erba was used for both syntheses (*i.e.*, reaction involving NOBF$_4$) and purifications by semi-preparative HPLC. Anhydrous DMSO was purchased from Carlo Erba, and stored over 3 Å molecular sieves, and UV-spectroscopy grade DMSO was provided by Honeywell Riedel-de-Haën. CHCl$_3$ (for spectroscopy, #167730010), purchased from Acros Organics, and absolute EtOH (>99.8%) from Honeywell Riedel-de Haën

were used for spectral measurements. TFA (HPLC grade, +99%) was provided by Fisher Chemical. Formic acid (FA, puriss p.a., ACS reagent, reag. Ph. Eur., ≥98%) was provided by Merck Millipore (Sigma-Aldrich brand). The HPLC-gradient grade MeCN was obtained from Carlo Erba or Fisher Chemical. All aqueous buffers used in this work and aqueous mobile-phases for HPLC were prepared using water purified with a PURELAB Ultra system from ELGA (purified to 18.2 MΩ.cm). 8-Bromojulolidine [64230-25-7], dimethyldiarylsilane DAEA-Si **6** [2101958-80-7] and aza-BODIPY dye (BF$_2$ chelate of [5-(4-methoxyphenyl)-3-phenyl-1H-pyrrol-2-yl]-[5-(4-methoxyphenyl)-3-phenyl-pyrrol-2-ylidene]-amine) [490035-88-6] were prepared according to literature procedures.[26-27, 43]

Instruments and methods
Freeze-drying operations were performed with a Christ Alpha 2-4 LD plus. Centrifugation steps were performed with a Thermo Scientific Espresso Personal Microcentrifuge instrument. ^{1}H-, ^{13}C- and ^{19}F-NMR spectra were recorded on a Bruker Avance Neo 500 MHz (equipped with a 5 mm BBOF iProbe). Chemical shifts are expressed in parts per million (ppm) from the residual non-deuterated solvent signal.[44] *J* values are expressed in Hz. IR spectra were recorded with a Bruker Alpha FT-IR spectrometer equipped with a universal ATR sampling accessory. The bond vibration frequencies are expressed in reciprocal centimeters (cm^{-1}). HPLC-MS analyses were performed on a Thermo-Dionex Ultimate 3000 instrument (pump + autosampler at 20 °C + column oven at 25 °C) equipped with a diode array detector (Thermo-Dionex DAD 3000-RS) and MSQ Plus single quadrupole mass spectrometer. Purifications by semi-preparative HPLC were performed on a Thermo-Dionex Ultimate 3000 instrument (semi-preparative pump HPG-3200BX) equipped with an RS Variable Detector (VWD-3400RS, four distinct wavelengths within the range 190-800 nm). Ion chromatography analyses (for the determination of TFA or BF$_4^-$ mass content in samples) were performed using a Thermo Scientific Dionex ICS 5000 ion chromatograph equipped with a conductivity detector CD (Thermo Scientific Dionex) and a conductivity suppressor ASRS-ultra II 4 mm (Thermo Scientific Dionex), and according to a method developed by the PACSMUB staff. Low-resolution mass spectra (LRMS) were recorded on a Thermo Scientific MSQ Plus single quadrupole equipped with an electrospray (ESI) source (LC-MS coupling). UV-visible spectra were obtained either on a Varian Cary 50 Scan or on a Agilent Cary 60 (single-beam) spectrophotometer (software Cary WinUV) by using a rectangular quartz cell (Hellma, 100-QS, 45 × 12.5 × 12.5 mm, pathlength: 10 mm, chamber volume: 3.5 mL), at 25 °C (using a temperature control system combined with water circulation). The absorption spectra of phenoxazine dyes were recorded in the corresponding solvent within the concentration range 5-20 µM (three distinct dilutions for the accurate determination of molar extinction coefficients). The vast majority of fluorescence spectra were recorded on an HORIBA Jobin Yvon Fluorolog spectrofluorometer (software FluorEssence) at 25 °C (using a temperature control system combined with water circulation), with a standard fluorometer cell (Labbox, LB Q, light path: 10 mm, width: 10 mm, chamber volume: 3.5 mL). The following set of parameters was used: shutter: Auto Open, Ex/Em slits = 5 nm for recording emission spectra and Ex/Em slits = 5 nm for recording excitation spectra, integration time = 0.1 s, 1 nm step, HV(S1) = 950 V. All fluorescence spectra were corrected. Relative fluorescence quantum yields were measured in the corresponding buffer at 25 °C by a relative method using the suitable standard (aza-BODIPY dye: Φ$_F$ = 36% in CHCl$_3$, excitation at 630 nm[43] or Nile Blue: Φ$_F$ = 27% in EtOH, excitation at 600 nm[33]; dilution by a factor ×3 between absorption and fluorescence measurements). The following equation was used to determine the relative fluorescence quantum yield:

$$\Phi_F(x) = (A_S/A_X)(F_X/F_S)(n_X/n_S)^2 \Phi_F(s)$$

where A is the absorbance (in the range of 0.01-0.1 A.U.), F is the area under the emission curve, n is the refractive index of the solvents (at 25 °C) used in measurements, and the subscripts s and x represent standard and unknown, respectively. The following refractive indices were used: 1.337 for PB, 1.333 for water, aq. 0.1% FA and HEPES buffer, 1.362 for EtOH, 1.489 for CHCl$_3$, and 1.478 for DMSO. Fluorescence-based kinetic assays were performed on a SAFAS Flx-Xenius XC spectrofluorimeter using quartz cells (SAFAS, Quartz Suprasil for SAFAS flx Xenius, 45 × 12.5 × 12.5 mm, pathlength: 10 mm, chamber volume: 3.5 mL), at 25 °C (using a temperature control system combined with water circulation). The following set of parameters was used: Ex/Em bandwidth = 5 nm, integration time = 0.5 s, and tunable PMT voltage. All fluorescence spectra were corrected.

High-performance liquid chromatography separations
Several chromatographic systems were used for the analytical experiments (HPLC-MS) and the purification steps: <u>System A:</u> RP-HPLC-

MS (Phenomenex Kinetex C$_{18}$ column, 2.6 µm, 2.1 × 50 mm) with MeCN (+0.1% FA) and 0.1% aqueous formic acid (aqueous FA, pH 2.1) as eluents [5% MeCN (0.1 min) followed by linear gradient from 5% to 100% (5 min) of MeCN, then 100% MeCN (1.5 min)] at a flow rate of 0.5 mL/min. UV-visible detection was achieved at 220, 260, 645 and 680 nm (+diode array detection in the range of 220-700 nm). Low resolution ESI-MS detection in the positive/negative mode (full scan, 100-1000 a.m.u., data type: centroid, needle voltage: 3.0 kV, probe temperature: 350 °C, cone voltage: 75 V and scan time: 1 s). System B: semi-preparative RP-HPLC (SiliCycle SiliaChrom C$_{18}$ column, 10 µm, 20 × 250 mm) with MeCN and aq. 0.1 TFA (pH 1.9) as eluents [10% MeCN (5 min), followed by a gradient of 10% to 20% MeCN (7.5 min), then 20% to 100% MeCN (93 min)] at a flow rate of 20.0 mL/min. Quadruple UV-visible detection was achieved at 220, 270, 645 and 700 nm. System C: RP-HPLC-fluorescence (Phenomenex Kinetex C$_{18}$ column, 2.6 µm, 2.1 × 50 mm) with same eluents and gradient as system A. Fluorescence detection was achieved at 45 °C at the following Ex/Em channels: 650/675 nm, and 685/730 nm (sensitivity: 1, PMT Auto, filter wheel: Auto). System D: system A with UV-visible detection at 220, 260, 650 and 680 nm (+diode array detection in the range 220-800 nm). Low resolution ESI-MS detection in the positive/negative modes (full scan, 100-1000 a.m.u., data type: centroid, needle voltage: 3.0 kV, probe temperature: 350 °C, cone voltage: 75 V and scan time: 1 s).

Syntheses

Bis(3-dimethylaminophenyl) ether 4 [867020-61-9]
A mixture of 3-(dimethylamino)phenol (162 mg, 1.18 mmol, 1 equiv.), 3-bromo-*N,N*-dimethylaniline (558 mg, 4.28 mmol, 3.6 equiv.), finely ground anhydrous K$_3$PO$_4$ (732 mg, 3.54 mmol, 3 equiv.), CuI (33 mg, 0.27 mmol, 0.15 equiv.) and picolinic acid (43 mg, 0.35 mmol, 0.3 equiv.) in dry DMSO (4.2 mL) was heated in a sealed tube at 130 °C overnight. The reaction was checked for completion by TLC (eluent: heptane/DCM 1:1, v/v) and diluted with EtOAc. Thereafter, the resulting organic phase was washed twice with brine, dried over anhydrous MgSO$_4$, filtered and concentrated under reduced pressure. The resulting residue was purified by flash-column chromatography over silica gel (eluent: heptane/DCM 1:1, v/v) to give the desired product as pinkish amorphous powder (227 mg, 0.89 mmol, yield 75%). IR (ATR): ν = 3061, 3028, 2884, 2844, 2799, 2209, 2073, 1950, 1924, 1885, 1605, 1576, 1563, 1496, 1442, 1356, 1324, 1228, 1168, 1151, 1123, 1062, 1004, 871, 850, 833, 449, 748, 725; ^{1}H NMR (500 MHz, CDCl$_3$): δ = 7.17 (t, *J* = 8.0 Hz, 2H), 6.52-6.43 (m, 4H), 6.37 (ddd, *J* = 8.0 Hz, *J* = 2.2 Hz, *J* = 0.8 Hz, 2H), 2.94 (s, 12H); ^{13}C NMR (126 MHz, CDCl$_3$): δ = 158.5, 152.2, 129.9, 107.5, 106.9, 103.5, 40.7; HPLC (system A): t_R = 4.2 min (purity >99% at 260 nm); LRMS (ESI+, recorded during RP-HPLC analysis): *m/z* 257.4 [M + H]$^+$ (100) and 298.4 [M +H + MeCN]$^+$ (70), calcd for C$_{16}$H$_{21}$N$_2$O$^+$ 257.2.

N-Oxide phenoxazine dye 7
To a solution of symmetrical diaryl ether analog 4 (100 mg, 0.39 mmol, 1 equiv.) in MeCN (5 mL), was added NOBF$_4$ (46 mg, 0.39 mmol, 1 equiv.). The resulting reaction mixture was stirred at RT for 5 min. Afterwards, the reaction mixture was concentrated under reduced pressure and the residue diluted with deionized H$_2$O. This aqueous mixture was extracted with DCM and DCM/iPrOH (1:1, v/v). The combined organic layers were dried over anhydrous MgSO$_4$, filtered and concentrated under reduced pressure. The resulting residue was purified by flash-column chromatography over silica gel (a step gradient of MeOH in DCM from 0% to 2%) to give the desired product as dark blue amorphous powder (36 mg, 97 µmol, yield 25% based on BF$_4^-$ mass = 23.6% determined by ionic chromatography). IR (ATR): ν = 3564, 3088, 2923, 1636, 1595, 1523, 1488, 1435, 1390, 1364, 1330, 1283, 1181, 1120, 1031, 928, 862, 825, 760; ^{1}H NMR (500 MHz, [D$_6$]DMSO): δ = 8.09 (d, *J* = 9.8 Hz, 2H), 7.29 (dd, *J* = 9.8 Hz, *J* = 2.6 Hz, 2H), 6.85 (d, *J* = 2.5 Hz, 2H), 3.32 (s, 12H); ^{13}C NMR (126 MHz, [D$_6$]DMSO): δ = 156.4, 152.0, 125.8, 122.3, 116.3, 95.7, 41.0; ^{19}F NMR (470 MHz, [D$_6$]DMSO): δ = -148.3 (d, *J* = 2.2 Hz, 4F, B*F$_4$*$^-$); HPLC (system A): t_R = 3.36 min (purity >97% at 260 nm, >99% at 645 nm and >99% at 680 nm); LRMS (ESI+, recorded during RP-HPLC analysis): *m/z* 284.4 [M]$^+$ (100), calcd for C$_{16}$H$_{18}$N$_3$O$_2^+$ 284.1.

Phenoxazine dye 8
To a solution of N-oxide phenoxazine dye 8 (15 mg, 40 µmol, 1 equiv.) in MeCN (1 mL), was added PPh$_3$ (13 mg, 0.05 mmol, 1.2 equiv.). The resulting reaction mixture was stirred at RT for 2 h. The reaction was checked for completion by RP-HPLC-MS (system A) and diluted with aq. 0.1% TFA. The resulting solution was directly purified by semi-preparative RP-HPLC (system B, t_R = 22.0-28.0 min). The product containing fractions were lyophilized to give the desired product as dark blue amorphous powder (14 mg, 26 µmol, yield 65% based on TFA mass = 50.04% determined by ionic chromatography). IR (ATR): ν = 2929, 1777, 1727,

1693, 1651, 1601, 1503, 1491, 1396, 1345, 1179, 1126, 1061, 912, 887, 855, 827, 787; ^{1}H NMR (500 MHz, [D$_6$]DMSO): δ = 7.79 (d, *J* = 9.6 Hz, 2H), 7.41 (dd, *J* = 9.6 Hz, *J* = 2.7 Hz, 2H), 6.93 (d, *J* = 2.7 Hz, 2H), 3.38 (s, 12H); ^{13}C NMR (126 MHz, [D$_6$]DMSO): δ = 157.2, 148.5, 133.8, 133.6, 117.6, 96.3, 41.3; ^{19}F NMR (470 MHz, D$_6$]DMSO): δ = -74.3 (s, 3F, C*F$_3$*-TFA); HPLC (system A): t_R = 3.25 min (purity >99% at 260 nm, >99% at 645 nm and >99% at 680 nm); LRMS (ESI+, recorded during RP-HPLC analysis): *m/z* 268.4 [M]$^+$ (100), calcd for C$_{16}$H$_{18}$N$_3$O$^+$ 268.1.

In vitro activation of "covalent-assembly fluorescent probe 4 by NO

Experimental details about stock solutions of probe and reactive analytes
- Solution A: a stock solution of probe 4 (1.0 mg/mL, 3.9 mM) in DMSO (UV-spectroscopy grade).
- Solution B: a 10.7 mM solution of NO, prepared according to the protocol described in the literature.[37a]
- Solution C: solution of TCEP (140 mM) in ultrapure H$_2$O, directly used without dilution. Commercial TCEP hydrochloride (Acros Organics, #363630010) was used to prepare this solution as follows: 4.92 mg in 1227 µL of ultrapure H$_2$O and subsequent neutralization with aq. 10 M NaOH.
- Solution D: solution of NADH (Sigma, #43420-1G, 140 mM) in ultrapure H$_2$O (6.62 mg in 666 µL), directly used without dilution.

Fluorescence-based assays
All assays were performed at 25 °C (using a temperature control system combined with water circulation) and conducted under continuous mechanical stirring through the use of small stirrer blades. Solution A (6.4 µL) was mixed with 2.5 mL of ultrapure water in 3.5 mL fluorescence quartz cell (final concentration of probe 4: 10 µM). Fluorescence emission at Ex/Em 685/730 nm (bandwidth = 5 nm, PMT = 600 V) was recorded every 10 s. After 5 min, the selected volume of solution B (corresponding to the number of NO equiv. to add) was added and the recording of NIR-I fluorescence signal continued for 15-20 min. Experiments involving sequential addition/incubation with NO and reducing agent (TCEP or NADH, solutions C and D) were achieved in the same manner but the detection of phenoxazine dye 8 also required the use of a second set of parameters Ex/Em 650/675 nm (bandwidth = 5 nm, PMT = 600 V, dual measurement at Ex/Em 685/730 nm and Ex/Em 650/675 nm respectively, every 25 s). Before and after each kinetic experiment, fluorescence emission spectrum (scan mode) of solution was recorded using the following parameters: Ex at 630 nm (bandwidth = 5 nm), Em within the range 640-950 nm (bandwidth = 5 nm), 1 nm step, full filtering, and average time = 0.1 s. *Please note: the availability of a 10 quartz cell rack on SAFAS Flx-Xenius XC spectrofluorimeter enables to achieve several kinetics at the same time.* Blank experiments to assess the stability of the probe 4 in H$_2$O and in presence of reducing agents, were achieved in the same way.

RP-HPLC-fluorescence and RP-HPLC-MS (full scan mode) analyses
Crude solutions from fluorescence-based assays were directly analyzed by RP-HPLC-fluorescence (injected volume: 10 µL, system C) and RP-HPLC-MS (injected volume: 20 µL, system D). Pure samples of N-oxide 7 and phenoxazine dye 8 (10 µM solution prepared in ultrapure H$_2$O) were analyzed under the same conditions. For "co-injection" analyses, 250 µL of crude solutions from fluorescence-based assays (*vide supra*) were combined to 250 µL of reference solutions (pure sample of 7 or 8), and 10 or 20 µL of the mix was injected into the HPLC-fluorescence/MS apparatus (systems C and D).

References

[1] For selected reviews, see: a) M. Ionescu, H. Mantsch, in *Advances in Heterocyclic Chemistry, Vol. 8* (Eds.: A. R. Katritzky, A. J. Boulton), Academic Press, **1967**, pp. 83-113; b) E. A. Onoabedje, S. A. Egu, M. A. Ezeokonkwo, U. C. Okoro, *J. Mol. Struct.* **2019**, *1175*, 956-962.

[2] For a comprehensive review, see: C. O. Okafor, *Dyes Pigm.* **1986**, *7*, 103-131.

[3] For a comprehensive review, see: V. Martinez, M. Henary, *Chem. - Eur. J.* **2016**, *22*, 13764-13782.

[4] For a comprehensive review, see: J. Jose, K. Burgess, *Tetrahedron* **2006**, *62*, 11021-11037.

[5] a) O. A. Kucherak, S. Oncul, Z. Darwich, D. A. Yushchenko, Y. Arntz, P. Didier, Y. Mely, A. S. Klymchenko, *J. Am. Chem. Soc.* **2010**, *132*, 4907-4916; b) Z. Darwich, A. S. Klymchenko, O. A. Kucherak, L. Richert, Y. Mely, *Biochim. Biophys. Acta, Biomembr.* **2012**, *1818*, 3048-3054; c) Z. Darwich, A. S. Klymchenko, D. Dujardin, Y. Mely, *RSC Adv.* **2014**, *4*, 8481-8488; d) I. A. Karpenko, R. Kreder, C. Valencia, P. Villa, C. Mendre, B. Mouillac, Y. Mely, M. Hibert, D. Bonnet, A. S. Klymchenko, *ChemBioChem* **2014**, *15*, 359-363; e) R. Saxena, S. Shrivastava, S. Haldar, A. S. Klymchenko, A. Chattopadhyay, *Chem. Phys. Lipids* **2014**, *183*, 1-8; f) R. Kreder, K. A. Pyrshev, Z. Darwich, O. A. Kucherak, Y. Mely, A. S. Klymchenko, *ACS Chem. Biol.* **2015**, *10*, 1435-1442; g) D. I. Danylchuk, S. Moon, K. Xu, A. S. Klymchenko, *Angew. Chem. Int. Ed.* **2019**, *58*, 14920-14924; h) D. I. Danylchuk, P.-H. Jouard, A. S. Klymchenko, *J. Am. Chem. Soc.* **2021**, *143*, 912-924; i) F. Hanser, C. Marsol, C. Valencia, P. Villa, A. S. Klymchenko, D. Bonnet, J. Karpenko, *ACS Chem. Biol.* **2021**, *16*, 651-660.

[6] M. Hintersteiner, A. Enz, P. Frey, A.-L. Jaton, W. Kinzy, R. Kneuer, U. Neumann, M. Rudin, M. Staufenbiel, M. Stoeckli, K.-H. Wiederhold, H.-U. Gremlich, *Nat. Biotechnol.* **2005**, *23*, 577-583.

[7] a) C. M. A. Alves, S. Naik, P. J. G. Coutinho, M. S. T. Gonçalves, *Tetrahedron* **2009**, *65*, 10441-10452; b) C. M. A. Alves, S. Naik, P. J. G. Coutinho, M. S. T. Gonalves, *Tetrahedron Lett.* **2011**, *52*, 112-116; c) B. Rama Raju, S. Naik, P. J. G. Coutinho, M. S. T. Gonçalves, *Dyes Pigm.* **2013**, *99*, 220-227; d) B. R. Raju, M. S. T. Gonçalves, P. J. G. Coutinho, *Spectrochim. Acta, Part A* **2017**, *171*, 1-9.

[8] a) K. I. E. McLuckie, Z. A. E. Waller, D. A. Sanders, D. Alves, R. Rodriguez, J. Dash, G. J. McKenzie, A. R. Venkitaraman, S. Balasubramanian, *J. Am. Chem. Soc.* **2011**, *133*, 2658-2663; b) S. D. Verma, N. Pal, M. K. Singh, H. Shweta, M. F. Khan, S. Sen, *Anal. Chem.* **2012**, *84*, 7218-7226; c) H. Bo, C. Wang, Q. Gao, H. Qi, C. Zhang, *Talanta* **2013**, *108*, 131-135; d) Z. Niknezhad, L. Hassani, D. Norouzi, *Mater. Sci. Eng., C* **2016**, *58*, 1188-1193; e) V. B. Tsvetkov, A. M. Varizhuk, S. A. Lizunova, T. A. Nikolenko, I. A. Ivanov, V. V. Severov, E. S. Belyaev, E. A. Shitikov, G. E. Pozmogova, A. V. Aralov, *Org. Biomol. Chem.* **2020**, *18*, 6147-6154.

[9] For a comprehensive review, see: Y. Tang, D. Lee, J. Wang, G. Li, J. Yu, W. Lin, J. Yoon, *Chem. Soc. Rev.* **2015**, *44*, 5003-5015.

[10] a) N.-H. Ho, R. Weissleder, C.-H. Tung, *Bioorg. Med. Chem. Lett.* **2006**, *16*, 2599-2602; b) N.-h. Ho, R. Weissleder, C.-H. Tung, *Tetrahedron*

2006, *62*, 578-585; c) N.-H. Ho, R. Weissleder, C.-H. Tung, *ChemBioChem* **2007**, *8*, 560-566; d) S. Chen, X. Li, H. Ma, *ChemBioChem* **2009**, *10*, 1200-1207; e) J. Lu, Y. Song, W. Shi, X. Li, H. Ma, *Sens. Actuators B* **2012**, *161*, 615-620; f) Q. Wan, Y. Song, Z. Li, X. Gao, H. Ma, *Chem. Commun.* **2013**, *49*, 502-504; g) L. Li, W. Shi, Z. Wang, Q. Gong, H. Ma, *Anal. Chem.* **2015**, *87*, 8353-8359; h) Q. Gong, L. Li, X. Wu, H. Ma, *Chem. Sci.* **2016**, *7*, 4694-4697; i) Q. Gong, W. Shi, L. Li, X. Wu, H. Ma, *Anal. Chem.* **2016**, *88*, 8309-8314; j) Y. Matsuoka, K. Ohkubo, T. Yamasaki, M. Yamato, H. Ohtabu, T. Shirouzu, S. Fukuzumi, K.-i. Yamada, *RSC Adv.* **2016**, *6*, 60907-60915; k) X. He, Y. Xu, W. Shi, H. Ma, *Anal. Chem.* **2017**, *89*, 3217-3221; l) Y. Hu, H. Li, W. Shi, H. Ma, *Anal. Chem.* **2017**, *89*, 11107-11112; m) Q. Diao, H. Guo, Z. Yang, W. Luo, T. Li, D. Hou, *Spectrochim. Acta, Part A* **2019**, *223*, 117284; n) H. Niu, B. Ni, K. Chen, X. Yang, W. Cao, Y. Ye, Y. Zhao, *Talanta* **2019**, *196*, 145-152; o) J. Wu, D. Su, C. Qin, W. Li, J. Rodrigues, R. Sheng, L. Zeng, *Talanta* **2019**, *201*, 111-118; p) X. Rong, Z.-Y. Xu, J.-W. Yan, Z.-Z. Meng, B. Zhu, L. Zhang, *Molecules* **2020**, *25*, 4718; q) X.-Z. Yang, X.-R. Wei, R. Sun, Y.-J. Xu, J.-F. Ge, *Spectrochim. Acta, Part A* **2020**, *226*, 117582.

[11] a) A. Loudet, C. Thivierge, K. Burgess, *Dojin News* **2011**, *137*, 1-7; b) J. Fan, J. Hu, P. Zhan, X. Peng, *Chem. Soc. Rev.* **2013**, *42*, 29-43.

[12] K. Kolmakov, E. Hebisch, T. Wolfram, L. A. Nordwig, C. A. Wurm, H. Ta, V. Westphal, V. N. Belov, S. W. Hell, *Chem. - Eur. J.* **2015**, *21*, 13344-13356.

[13] a) J. Jose, K. Burgess, *J. Org. Chem.* **2006**, *71*, 7835-7839; b) J. Han, J. Jose, E. Mei, K. Burgess, *Angew. Chem. Int. Ed.* **2007**, *46*, 1684-1687; c) J. Jose, Y. Ueno, K. Burgess, *Chem. - Eur. J.* **2009**, *15*, 418-423; d) J. Jose, A. Loudet, Y. Ueno, R. Barhoumi, R. C. Burghardt, K. Burgess, *Org. Biomol. Chem.* **2010**, *8*, 2052-2059.

[14] a) V. H. J. Frade, M. S. T. Gonçalves, J. C. V. P. Moura, *Tetrahedron Lett.* **2005**, *46*, 4949-4952; b) V. H. J. Frade, M. S. T. Gonçalves, J. C. V. P. Moura, *Tetrahedron Lett.* **2006**, *47*, 8567-8570; c) V. H. J. Frade, S. A. Barros, J. C. V. P. Moura, P. J. G. Coutinho, M. S. T. Gonçalves, *Tetrahedron* **2007**, *63*, 12405-12418; d) V. H. J. Frade, S. A. Barros, J. C. V. P. Moura, M. S. T. Gonçalves, *Tetrahedron Lett.* **2007**, *48*, 3403-3407; e) V. H. J. Frade, P. J. G. Coutinho, J. C. V. P. Moura, M. S. T. Gonçalves, *Tetrahedron* **2007**, *63*, 1654-1663; f) V. H. J. Frade, M. S. T. Gonçalves, P. J. G. Coutinho, J. C. V. P. Moura, *J. Photochem. Photobiol., A* **2007**, *185*, 220-230; g) A. D. G. Firmino, M. S. T. Gonçalves, *Tetrahedron Lett.* **2012**, *53*, 4946-4950; h) B. R. Raju, A. M. F. Garcia, A. L. S. Costa, P. J. G. Coutinho, M. S. T. Gonçalves, *Dyes Pigm.* **2014**, *110*, 203-213; i) B. R. Raju, M. M. T. Carvalho, M. I. P. S. Leitão, P. J. G. Coutinho, M. S. T. Gonçalves, *Dyes Pigm.* **2016**, *132*, 204-212.

[15] a) S. M. Pauff, S. C. Miller, *Org. Lett.* **2011**, *13*, 6196-6199; b) A. Choi, S. C. Miller, *Org. Lett.* **2018**, *20*, 4482-4485.

[16] X. Luo, L. Gu, X. H. Qian, Y. C. Yang, *Chem. Commun.* **2020**, *56*, 9067-9078.

[17] Q. Zhang, Z. Zhu, Y. Zheng, J. Cheng, N. Zhang, Y.-T. Long, J. Zheng, X. Qian, Y. Yang, *J. Am. Chem. Soc.* **2012**, *134*, 18479-18482.

[18] J. Zhang, X. Chai, X.-P. He, H.-J. Kim, J. Yoon, H. Tian, *Chem. Soc. Rev.* **2019**, *48*, 683-722.

[19] a) Y. Yang, S. K. Seidlits, M. M. Adams, V. M. Lynch, C. E. Schmidt, E. V. Anslyn, J. B. Shear, *J. Am. Chem. Soc.* **2010**, *132*, 13114-13116; b) Y. Shen, Q. Zhang, X. Qian, Y. Yang, *Anal. Chem.* **2015**, *87*, 1274-1280; c) P. R. Escamilla, Y. Shen, Q. Zhang, D. S. Hernandez, C. J. Howard, X. Qian, D. Y. Filonov, A. V. Kinev, J. B. Shear, E. V. Anslyn, Y. Yang, *Chem. Sci.* **2020**, *11*, 1394-1403; d) Y. Yu, X. Zhang, Y. Dong, X. Luo, X. Qian, Y. Yang, *Sens. Actuators B* **2021**, *346*, 130562.

[20] a) S. Debieu, A. Romieu, *Org. Biomol. Chem.* **2017**, *15*, 2575-2584; b) S. Debieu, A. Romieu, *Tetrahedron Lett.* **2018**, *59*, 1940-1944; c) K. Renault, S. Debieu, J.-A. Richard, A. Romieu, *Org. Biomol. Chem.* **2019**, *17*, 8918-8932.

[21] W. A. Prütz, *J. Chem. Soc., Chem. Commun.* **1994**, 1639-1640.

[22] L. Wang, J. Liu, S. Zhao, H. Zhang, Y. Sun, A. Wei, W. Guo, *Chem. Commun.* **2020**, *56*, 7718-7721.

[23] a) Y. Koide, Y. Urano, K. Hanaoka, T. Terai, T. Nagano, *ACS Chem. Biol.* **2011**, *6*, 600-608; b) Y. Koide, Y. Urano, K. Hanaoka, W. Piao, M. Kusakabe, N. Saito, T. Terai, T. Okabe, T. Nagano, *J. Am. Chem. Soc.* **2012**, *134*, 5029-5031.

[24] For a comprehensive review, see: L. Wang, W. Du, Z. Hu, K. Uvdal, L. Li, W. Huang, *Angew. Chem., Int. Ed.* **2019**, *58*, 14026-14043.

[25] A. V. Anzalone, T. Y. Wang, Z. Chen, V. W. Cornish, *Angew. Chem. Int. Ed.* **2013**, *52*, 650-654.

[26] G. Dejouy, K. Renault, I. E. Valverde, A. Romieu, *Dyes Pigm.* **2020**, *180*, Article 108496.

[27] F. Deng, L. Liu, W. Huang, C. Huang, Q. Qiao, Z. Xu, *Spectrochim. Acta, Part A* **2020**, *240*, 118466.

[28] G. A. Olah, G. K. Surya Prakash, Q. Wang, X.-y. Li, G. K. Surya Prakash, J. Hu, in *Encyclopedia of Reagents for Organic Synthesis*, **2004**.

[29] a) A. Chevalier, J. Hardouin, P.-Y. Renard, A. Romieu, *Org. Lett.* **2013**, *15*, 6082-6085; b) A. Chevalier, C. Massif, P.-Y. Renard, A. Romieu, *Chem. - Eur. J.* **2013**, *19*, 1686-1699; c) A. Chevalier, C. Mercier, L. Saurel, S. Orenga, P.-Y. Renard, A. Romieu, *Chem. Commun.* **2013**, *49*, 8815-8817; d) A. Chevalier, P.-Y. Renard, A. Romieu, *Org. Lett.* **2014**, *16*, 3946-3949; e) A. Chevalier, W. Piao, K. Hanaoka, T. Nagano, P.-Y. Renard, A. Romieu, *Methods Appl. Fluoresc.* **2015**, *3*, 044004; f) M.-D. Hoang, J.-B. Bodin, F. Savina, V. Steinmetz, J. Bignon, P. Durand, G. Clavier, R. Méallet-Renault, A. Chevalier, *RSC Adv.* **2021**, *11*, 30088-30092.

[30] R. M. DeBaun, G. de Stevens, *Arch. Biochemi. Biophys.* **1951**, *31*, 300-308.

[31] E. Howard, W. F. Olszewski, *J. Am. Chem. Soc.* **1959**, *81*, 1483-1484.

[32] K. Rurack, M. Spieles, *Anal. Chem.* **2011**, *83*, 1232-1242.

[33] A. M. Brouwer, *Pure Appl. Chem.* **2011**, *83*, 2213-2228.

[34] C. Bueno, M. L. Villegas, S. G. Bertolotti, C. M. Previtali, M. G. Neumann, M. V. Encinas, *Photochem. Photobiol.* **2002**, *76*, 385-390.

[35] For a selected review, see: A. K. Vidanapathirana, P. J. Psaltis, C. A. Bursill, A. D. Abell, S. J. Nicholls, *Med. Res. Rev.* **2021**, *41*, 435-463.

[36] a) N. Kumar, V. Bhalla, M. Kumar, *Coord. Chem. Rev.* **2013**, *257*, 2335-2347; b) H. Li, A. Wan, *Analyst* **2015**, *140*, 7129-7141; c) Y. Chen, *Nitric Oxide* **2020**, *98*, 1-19; d) L. Wang, J. Zhang, X. An, H. Duan, *Org. Biomol. Chem.* **2020**, *18*, 1522-1549.

[37] a) K.-J. Huang, H. Wang, M. Ma, X. Zhang, H.-S. Zhang, *Nitric Oxide* **2007**, *16*, 36-43; b) R. Barbosa, A. Lopes, R. Santos, C. Pereira, C. Lourenço, B. Rocha, N. R. Ferreira, A. Ledo, J. Laranjinha, *Global J. Anal. Chem.* **2011**, *2*, 272-284.

[38] R. Tanikaga, *Bull. Chem. Soc. Jpn* **1968**, *41*, 1664-1668.

[39] a) T. M. Kitson, *Bioorg. Chem.* **1998**, *26*, 63-73; b) T. M. Kitson, K. E. Kitson, G. J. King, in *Adv. Exp. Med. Biol., Vol. 463* (Eds.: H. Weiner, E. MAser, D. W. Crabb, R. Lindahl), Springer, New York, **1999**, pp. 89-96.

[40] For a comprehensive review on cysteine-mediated redox signaling, see: C. E. Paulsen, K. S. Carroll, *Chem. Rev.* **2013**, *113*, 4633-4679.

[41] a) Y.-Q. Sun, J. Liu, H. Zhang, Y. Huo, X. Lv, Y. Shi, W. Guo, *J. Am. Chem. Soc.* **2014**, *136*, 12520-12523; b) X.-X. Chen, L.-Y. Niu, N. Shao, Q.-Z. Yang, *Anal. Chem.* **2019**, *91*, 4301-4306.

[42] N. Vijay, S. P. Wu, S. Velmathi, *ACS Appl. Bio Mater.* **2021**, *4*, 7007-7015.

[43] A. Gorman, J. Killoran, C. O'Shea, T. Kenna, W. M. Gallagher, D. F. O'Shea, *J. Am. Chem. Soc.* **2004**, *126*, 10619-10631.

[44] G. R. Fulmer, A. J. M. Miller, N. H. Sherden, H. E. Gottlieb, A. Nudelman, B. M. Stoltz, J. E. Bercaw, K. I. Goldberg, *Organometallics* **2010**, *29*, 2176-2179.

9
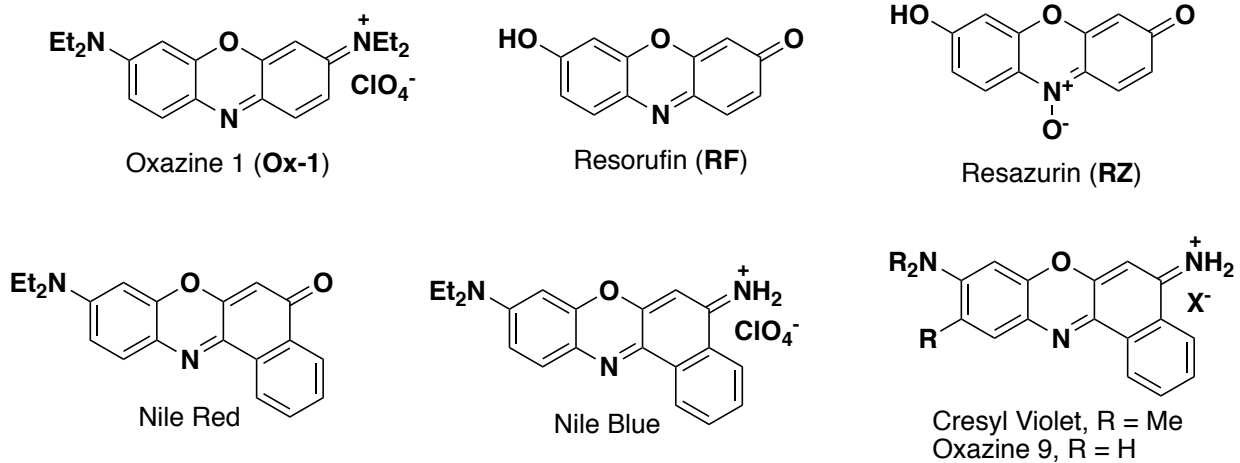
Figure 1. Structures of the most popular phenoxazine dyes currently used in fluorescence-based applications (X^- = Cl^- or ClO_4^-).
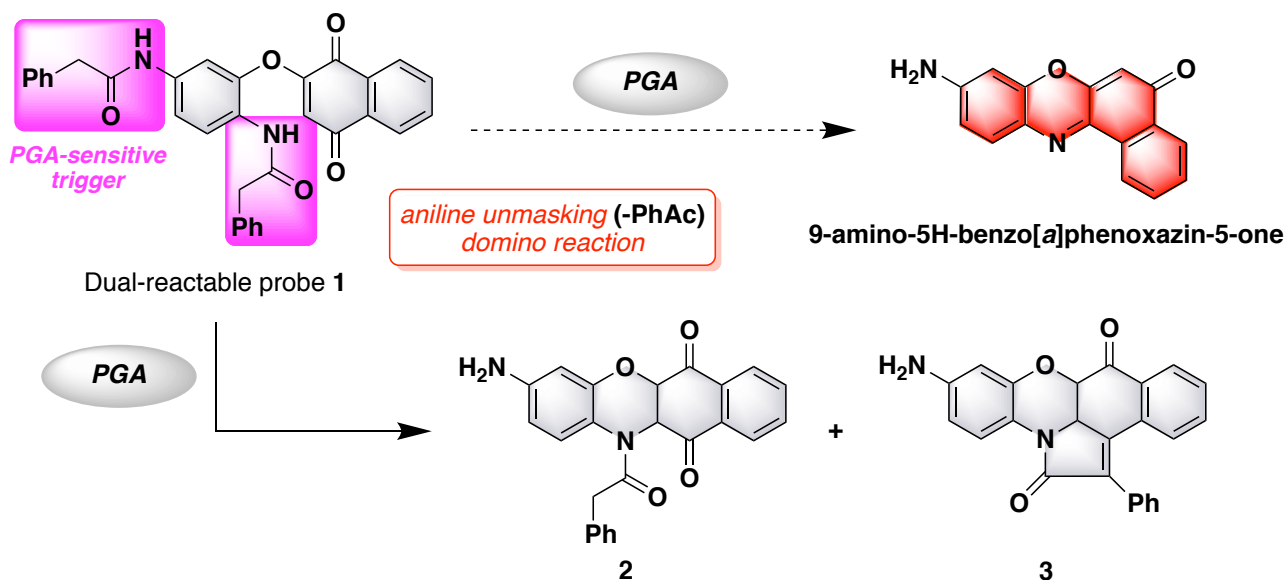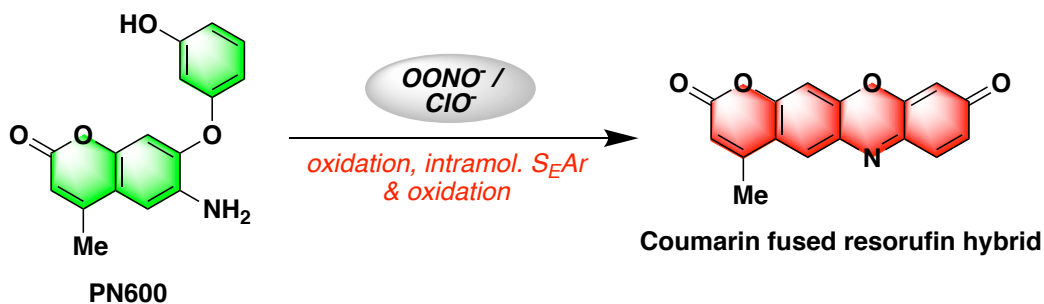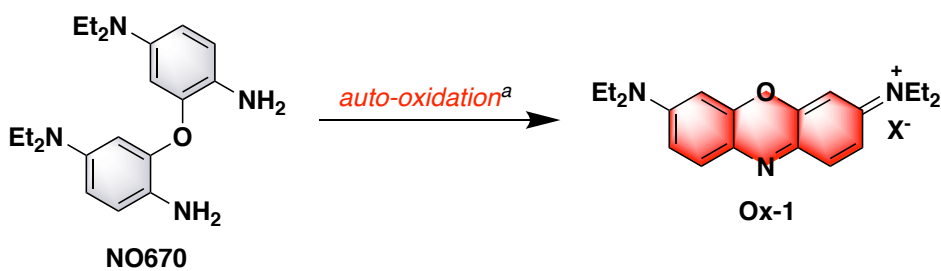
Figure 2. Overview of "covalent-assembly" fluorescent probes reported in the literature, whose activation leads to the *in situ* formation of phenoxazine dyes or related analogs [ClO⁻ = hypochlorite anion, OONO⁻ = peroxynitrite anion, PGA = penicillin G acylase, PhAc = phenylacetyl, X⁻ = counter ion not specified]. [a]Please note: the proneness of probe **NO670** to auto-oxidation mitigated its potential for practical applications. Synthesis of **NO670** and mechanistic studies related to its conversion into **Ox-1** were not published by the Yang group but only mentioned in their review on the "covalent-assembly" principle for fluorescent probe design[16].
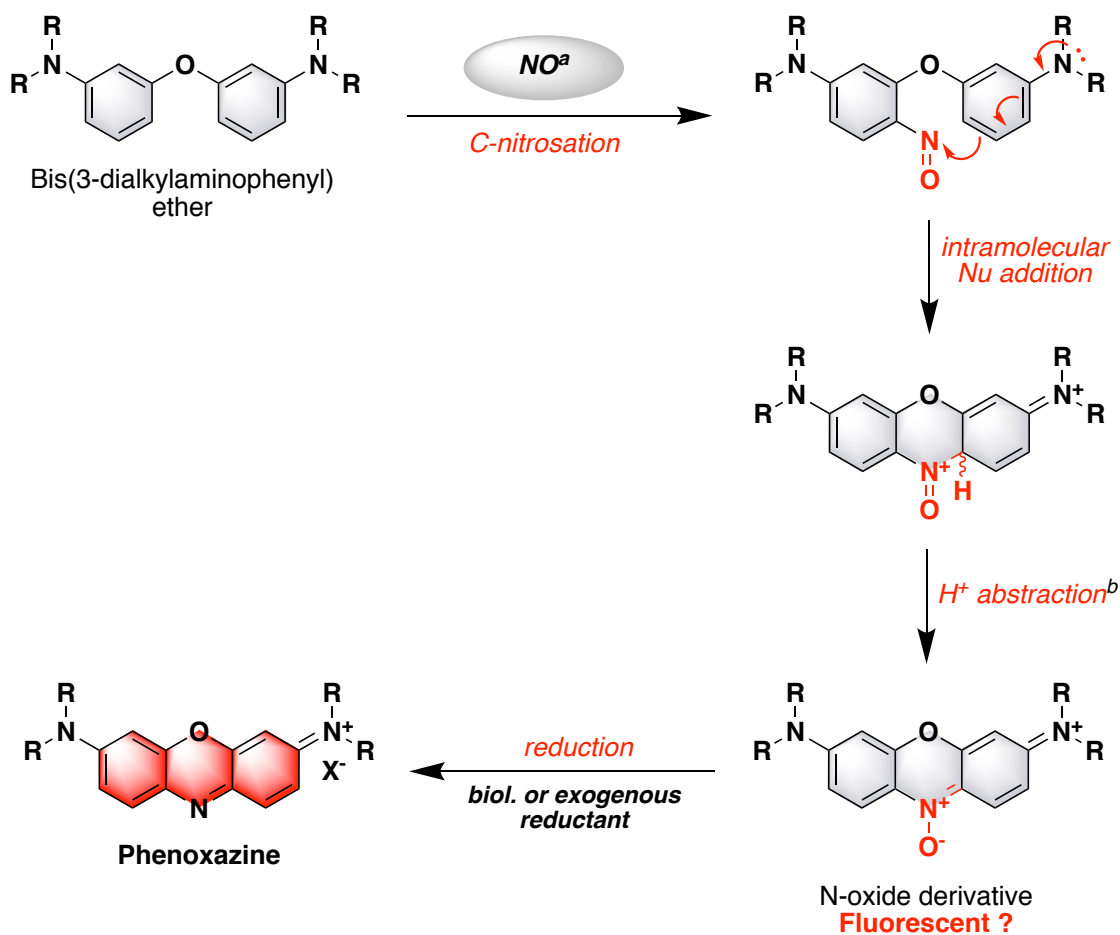
Figure 3. NO-sensing strategy explored in this work based on the use of "covalent-assembly" fluorogenic probes whose activation leads to the *in situ* formation of phenoxazine dyes [biol. = biological, Nu = nucleophilic, R = alkyl substituent, X⁻ = counter ion not specified]. [a]Please note: depending the context, the nitrosating species is different: NO^+ in the case of syntheses using $NOBF_4$ and probably N_2O_3 (itself in equilibrium with NO^+ and NO_2^-) in the case of experiments performed with freshly prepared aq. solution of nitric oxide. [b]Please note: depending the context, proton abstraction may be assisted by various species: BF_4^- anion, H_2O molecule, NO_2^- anion or N-oxide derivative itself.
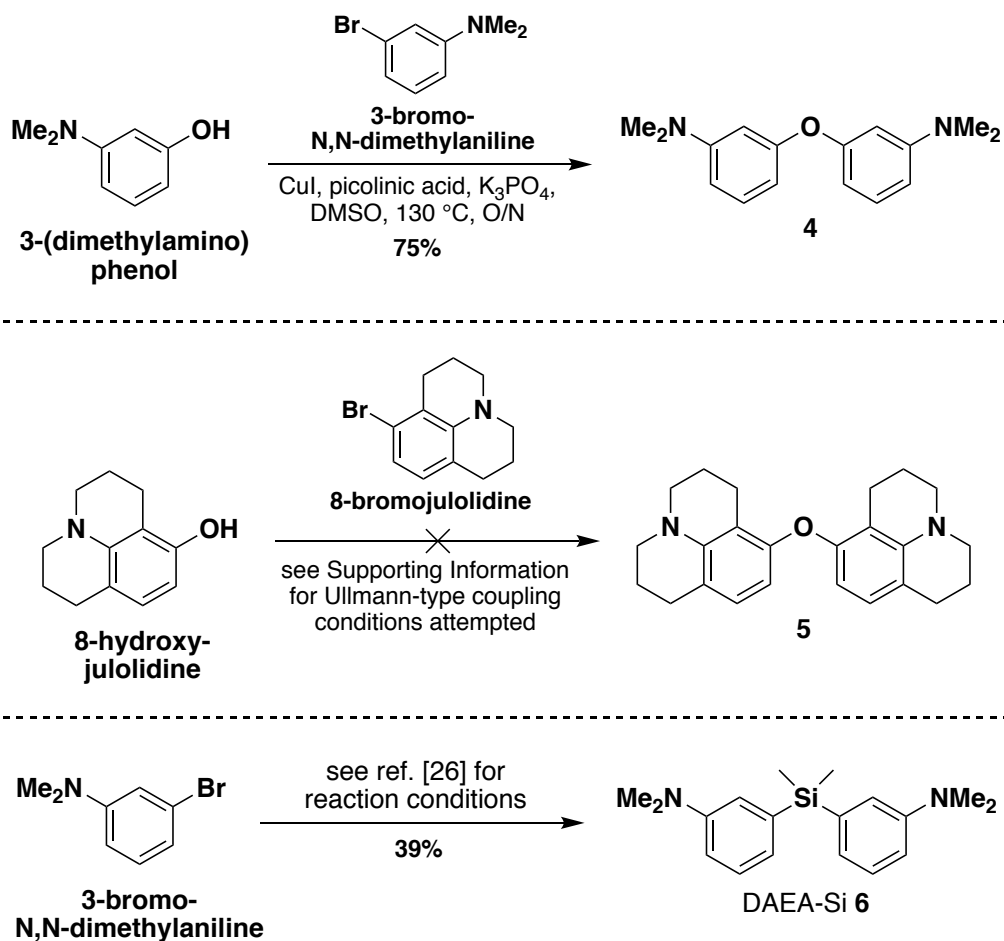
Scheme 1. Synthesis of symmetrical bis-aryl ethers **4** and **5** and the silicon-containing analog DAEA-Si **6**. [O/N = overnight].
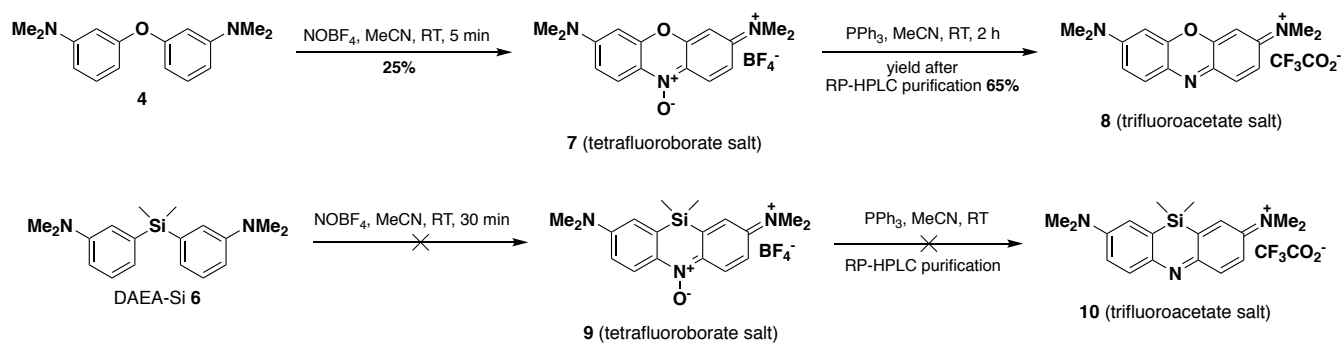
Scheme 2. Synthesis of phenoxazine dye **8** and its silicon analog **10** through NOBF₄-mediated nitrosation. [RT = room temperature].
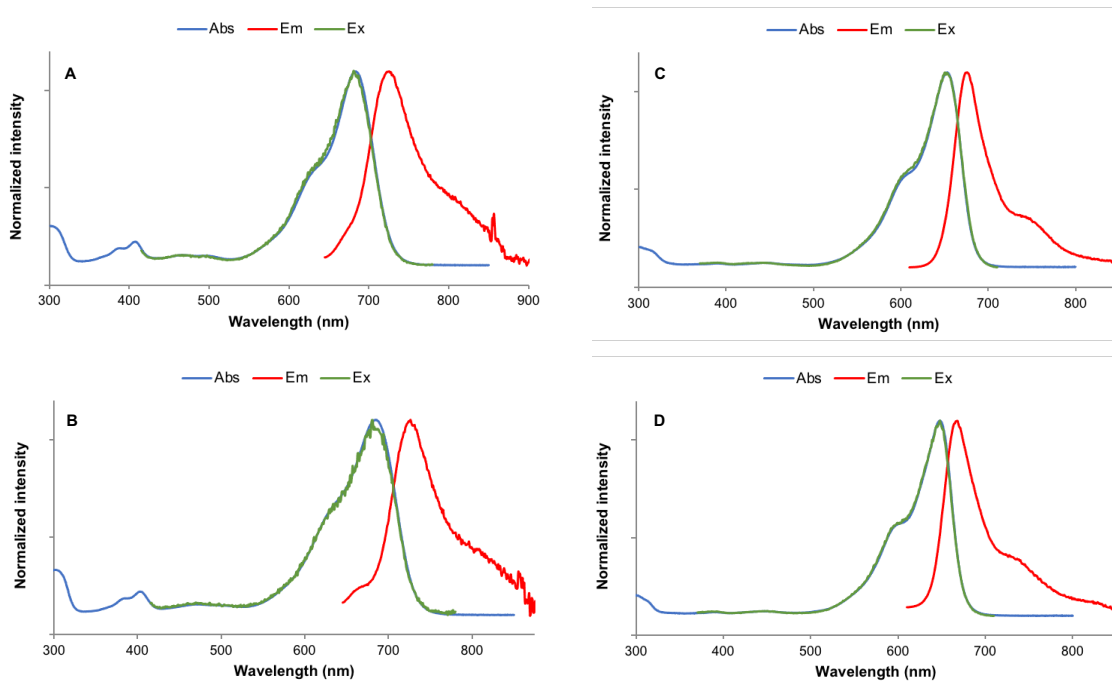
Figure 4. Normalized absorption, fluorescence emission (excitation at 630 nm (A-B) or 600 nm (C-D), Ex/Em slits 5 nm) and excitation (emission at 800 nm (A-B) or 720 nm (C-D), Ex/Em slits 5 nm) spectra of phenoxazine dyes **7** and **8** in DMSO (A, C), and in ultrapure water (B, D) at 25 °C.
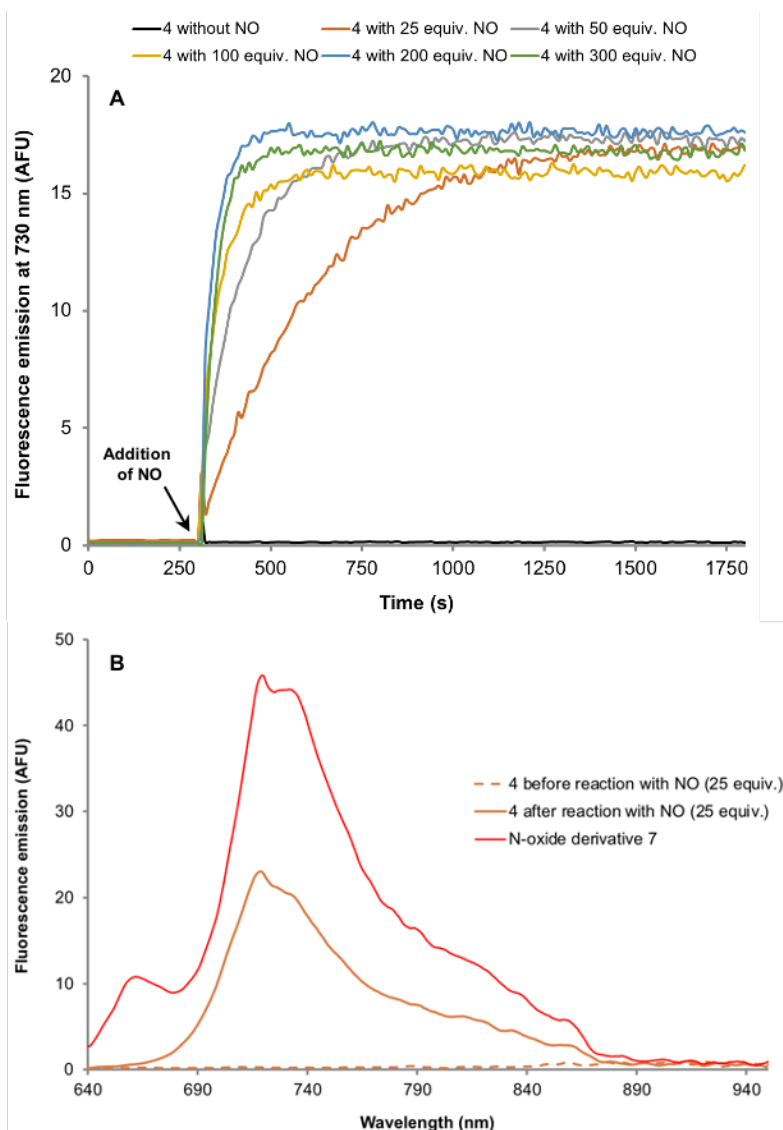
Figure 5. (A) Fluorescence emission time course (Ex/Em 685/730 nm, bandwidth 5 nm, PMT voltage 600 V) of "covalent-assembly" fluorogenic probe **4**, concentration: 10 μM, in the presence of various amounts of NO, in ultrapure water at 25 °C. (B) Overlay of fluorescence emission spectra (Ex at 630 nm, bandwidth 5 nm, PMT voltage 600 V) of "covalent-assembly" fluorogenic probe **4** before and after 25 min incubation with NO (25 equiv.), and N-oxide derivative **7** (reference sample synthesized from **4** with NOBF₄, see Scheme 2) at the same concentration (10 μM) in ultrapure water at 25 °C. <u>Please note</u>: the presented kinetics and emission curves were recorded with a SAFAS Flx-Xenius XC spectrofluorimeter, an instrument that is well suited for high-throughput measurements (*e.g.*, 10 different kinetics at the same time) but providing lower performances than HORIBA Jobin Yvon Fluorolog in the NIR-I spectral range; this explains the poorer quality of emission spectra compared to those presented in Figure 4. The minor band centered at 660 nm and observed in the emission spectrum of reference sample of **7**, is assigned to phenoxazine **8**, formed through a not yet elucidated (photo)reduction process occurring during the prolonged storage of **7** in solution (*i.e.*, 1.0 mg/mL stock solution in DMSO).
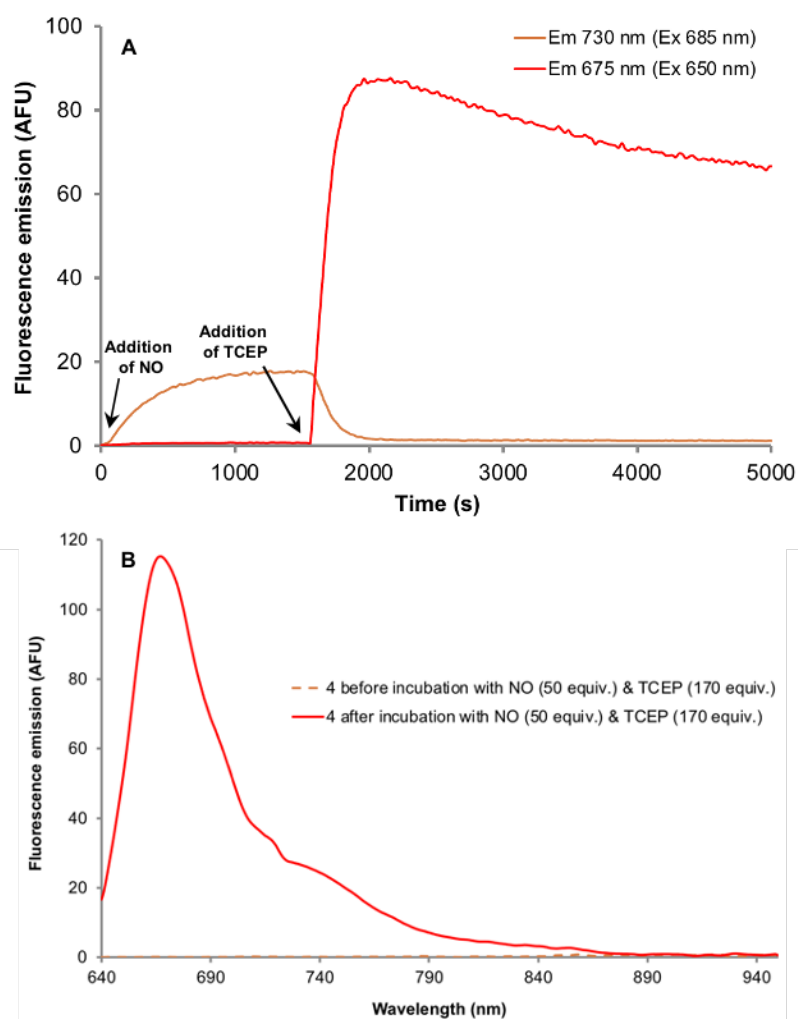
Figure 6. (A) Fluorescence emission time course (channel 1: Ex/Em 685/730 nm for **7**, channel 2: Ex/Em 650/675 nm for **8**; bandwidth 5 nm, PMT voltage 600 V) of "covalent-assembly" fluorogenic probe **4**, concentration: 10 μM, sequentially incubated with NO (50 equiv.) and TCEP (170 equiv.), in ultrapure water at 25 °C. (B) Fluorescence emission spectra (Ex at 630 nm, bandwidth 5 nm, PMT voltage 600 V) of "covalent-assembly" fluorogenic probe **4**, concentration: 10 μM, before and after sequential incubation with NO (50 equiv.) and TCEP (170 equiv.), in ultrapure water at 25 °C.
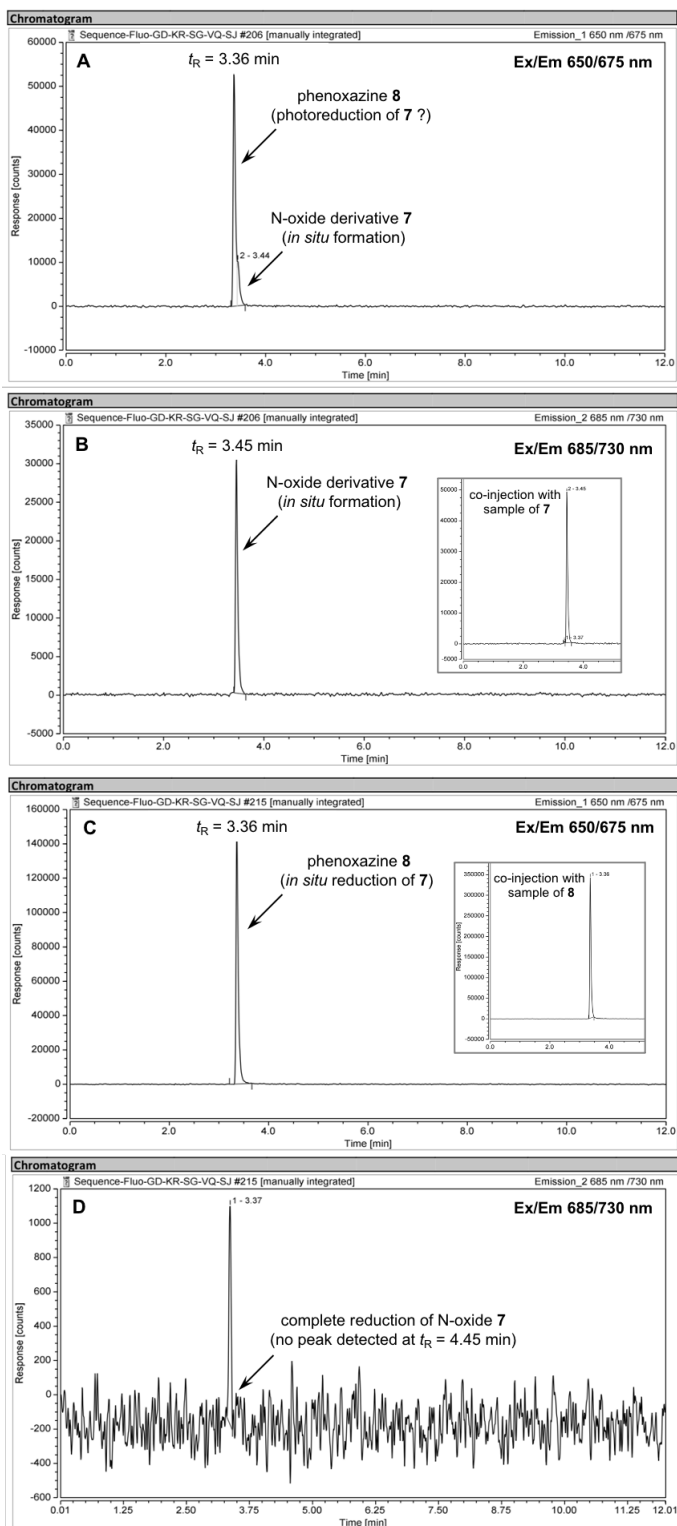
Figure 7. RP-HPLC elution profiles (system C, fluorescence detection in two distinct channels: Ex/Em 650/675 nm and Ex/Em 685/730 nm) of reaction mixtures of "covalent-assembly" fluorogenic probe **4** with NO (50 equiv.) for 25 min at 25 °C (A-B), or with NO (50 equiv., 25 min of incubation) and TCEP (170 equiv., 60 min of incubation) at 25 °C (C-D). Please note: see inset of (B) and (C) for co-injection analysis of the corresponding reaction mixture with an authentic sample of **7** or **8**.
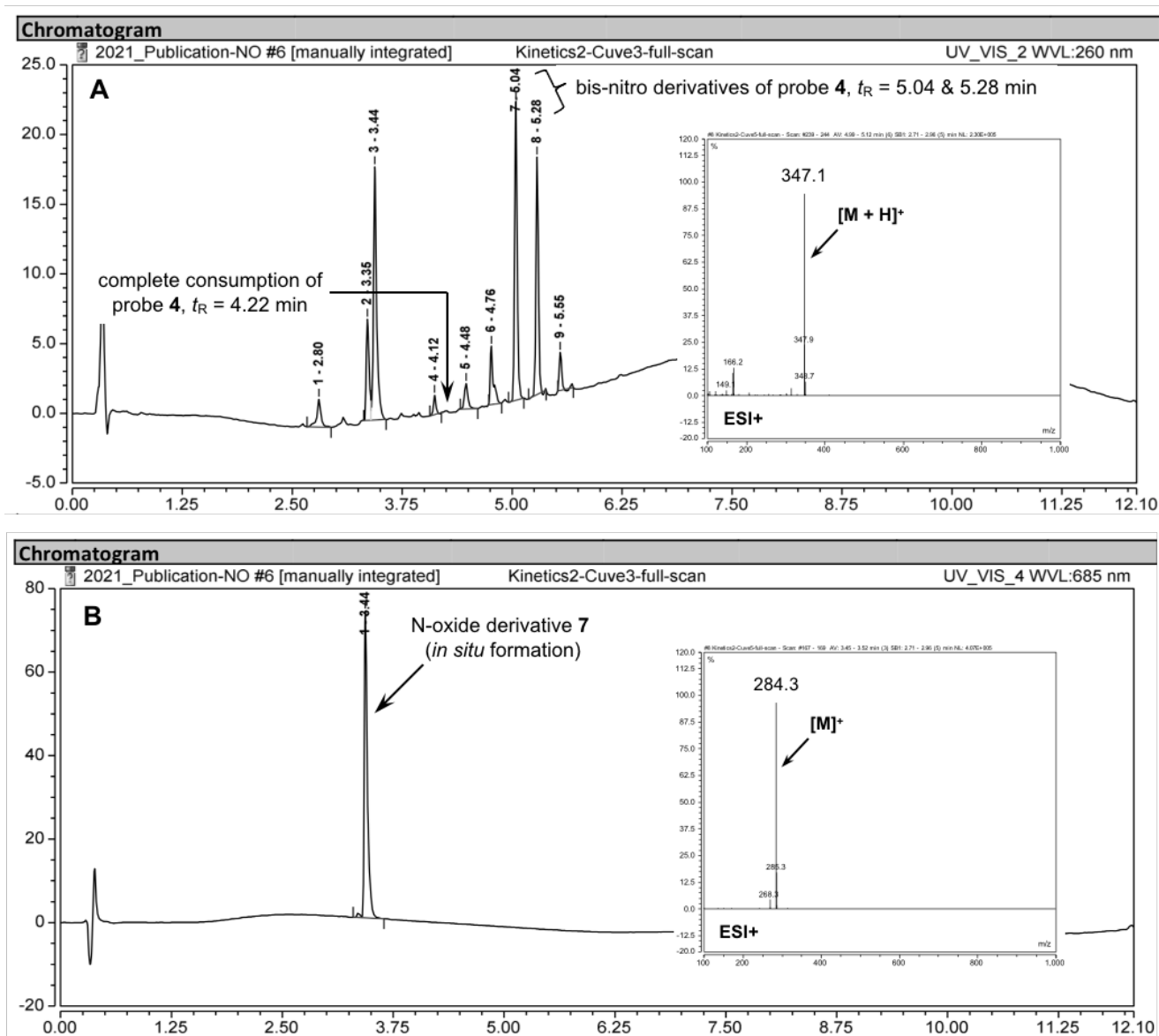
Figure 8. RP-HPLC elution profiles (system D) of "covalent-assembly" fluorogenic probe **4** after 25 min incubation with NO (50 equiv.) in ultrapure water at 25 °C. (A) UV detection at 260 nm and ESI+ mass spectrum of peaks at t_R = 5.04 and 5.28 min (inset). (B) Visible detection at 685 nm and ESI+ mass spectrum of peak at t_R = 3.44 min (inset).
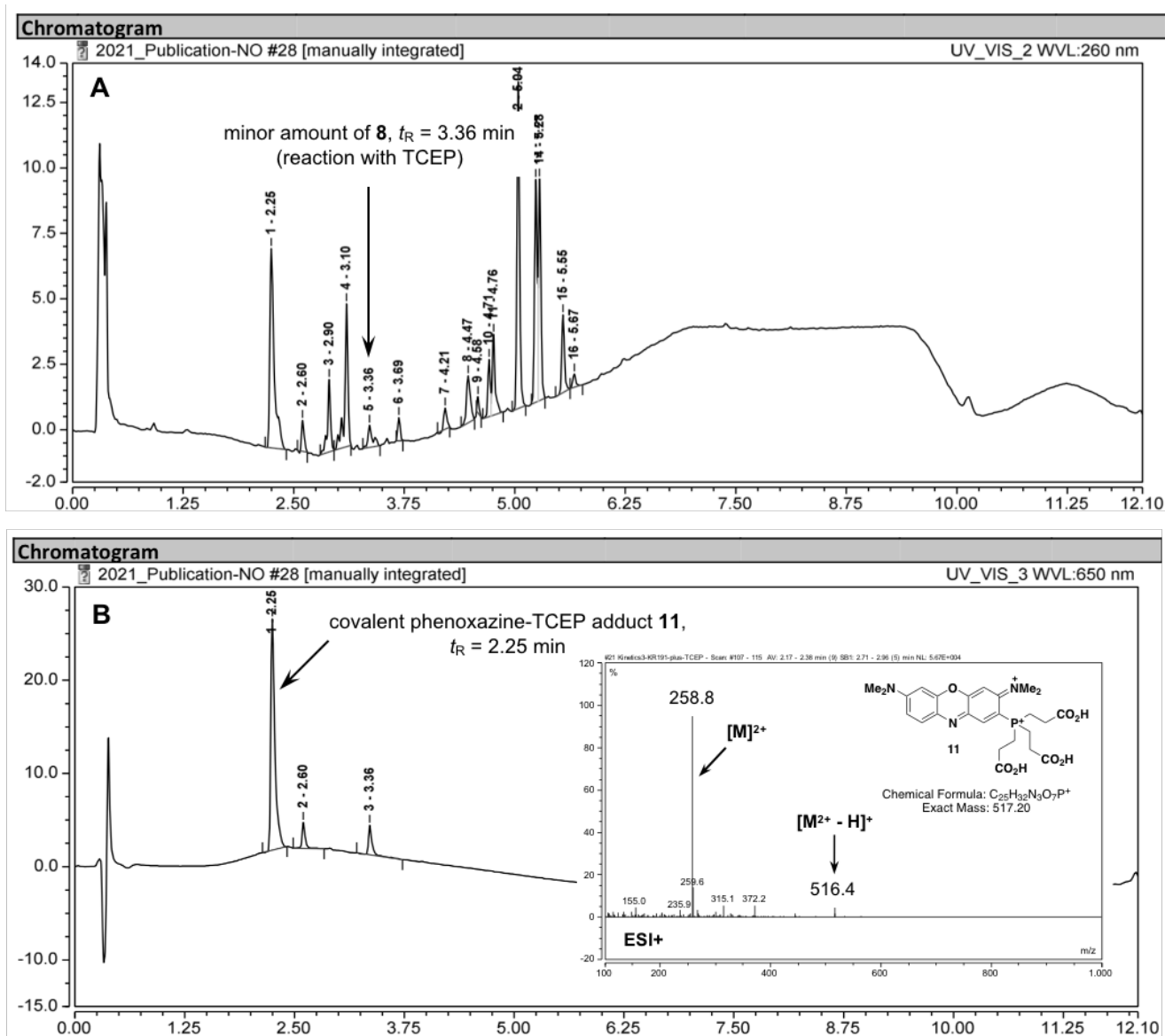
Figure 9. RP-HPLC elution profiles (system D) of "covalent-assembly" fluorogenic probe **4** after sequential incubation with NO (50 equiv., 25 min of incubation) and TCEP (170 equiv., 60 min of incubation) in ultrapure water, at 25 °C. (A) UV detection at 260 nm. (B) Visible detection at 650 nm and ESI+ mass spectrum of peak at t_R = 2.25 min (inset).
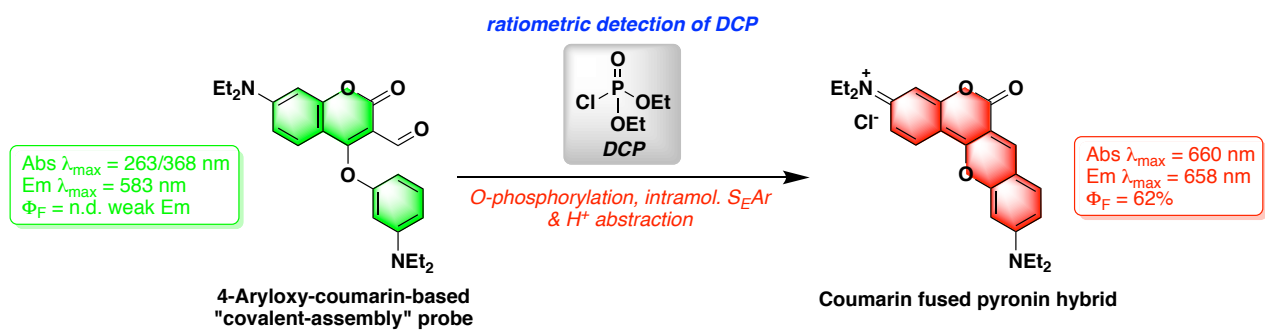
Figure 10. "Covalent-assembly" fluorescent probe recently reported by Vijay *et al.*[42] for ratiometric detection of nerve-agent mimic DCP [diethyl chlorophosphate] within the NIR-I spectral range. Please note: spectral features of probe and *in situ* formed coumarin fused pyronin hybrid dye were determined in DMSO.
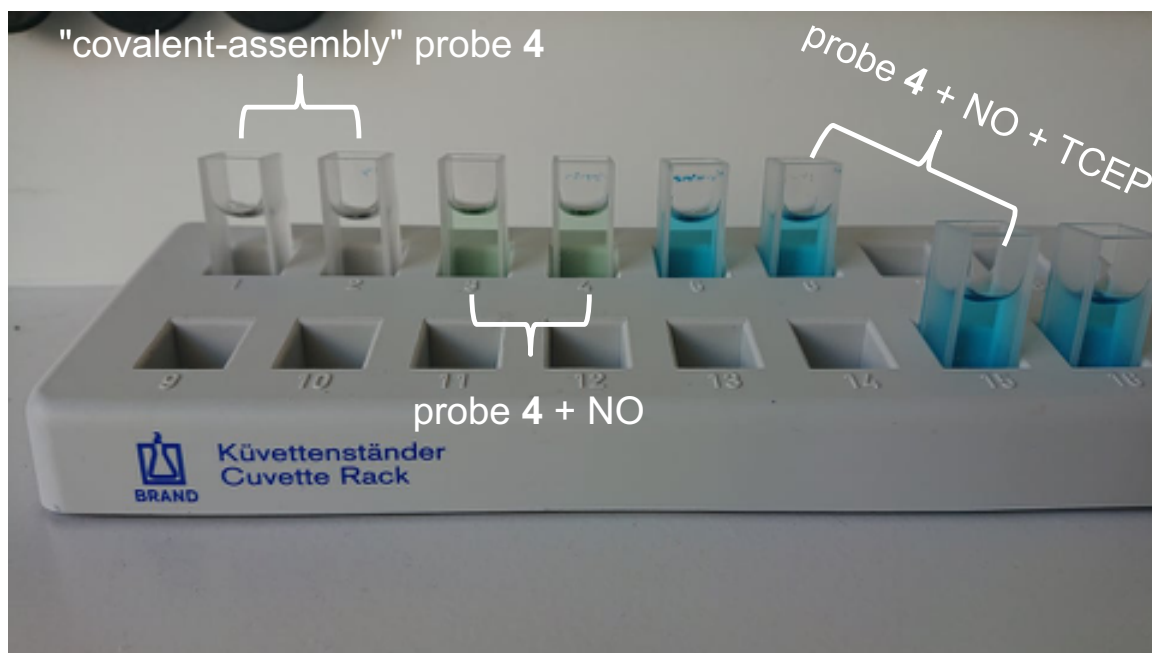
Figure S1. Picture of aq. solutions of "covalent-assembly" fluorogenic probe **4** before and after incubation with either NO (50 equiv.) or NO (50 equiv.) and TCEP (170 equiv.).